

AD-A072 414

NAVAL POSTGRADUATE SCHOOL MONTEREY CA

F/G 13/10

AN EXPERIMENTAL STUDY OF DROPWISE CONDENSATION ON HORIZONTAL CO--ETC(U)

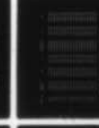
JUN 79 J T MANVEL

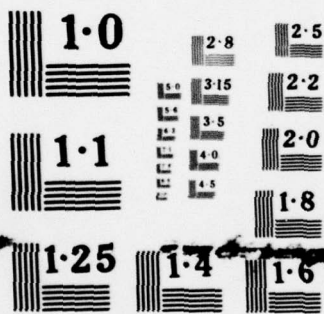
UNCLASSIFIED

NPS-69-79-004

NL

1 OF 2
AD
A072414





NATIONAL BUREAU OF STANDARDS
MICROCOPY RESOLUTION TEST CHART

AD A 072414

LEVEL

NPS 69-79-004

NAVAL POSTGRADUATE SCHOOL
Monterey, California

2



DDC
RECEIVED
AUG 7 1979
C

THESIS

DDC FILE COPY

AN EXPERIMENTAL STUDY OF
DROPWISE CONDENSATION ON
HORIZONTAL CONDENSER TUBES

by

John Talbot Manvel, Jr.

June 1979

Thesis Advisor:

P. J. Marto

Approved for public release; distribution unlimited.

Prepared for:

Naval Sea Systems Command
Washington, D. C.

79 08 06 018

NAVAL POSTGRADUATE SCHOOL
Monterey, California

Rear Admiral T. F. Dedman
Superintendent

Jack R. Borsting
Provost

This thesis prepared in conjunction with research supported
in part by the Naval Sea Systems Command under work request
N0002479-WR9G078.

Reproduction of all or part of this report is authorized.

Released as a
Technical Report by:

William M. Tolles
W. M. Tolles
Dean of Research

Accession For	
NTIS GRA&I	<input checked="checked" type="checkbox"/>
DDC TAB	<input type="checkbox"/>
Unannounced	<input type="checkbox"/>
Justification	
By _____	
Distribution/	
Availability Codes	
Dist	Avail and/or special

79 08 06 018

UNCLASSIFIED

SECURITY CLASSIFICATION OF THIS PAGE (When Data Entered)

REPORT DOCUMENTATION PAGE		READ INSTRUCTIONS BEFORE COMPLETING FORM
1. REPORT NUMBER (14) NPS-69-79-004	2. GOVT ACCESSION NO.	3. RECIPIENT'S CATALOG NUMBER
4. TITLE (and Subtitle) (6) An Experimental Study of Dropwise Condensation on Horizontal Condenser Tubes	5. TYPE OF REPORT & PERIOD COVERED (9) Master's Thesis June 1979	6. PERFORMING ORG. REPORT NUMBER
7. AUTHOR(s) (10) John Talbot/Manvel, Jr. and Paul J. Marto	8. CONTRACT OR GRANT NUMBER(s)	
9. PERFORMING ORGANIZATION NAME AND ADDRESS Naval Postgraduate School Monterey, California 93940	10. PROGRAM ELEMENT, PROJECT, TASK AREA & WORK UNIT NUMBERS N0002479-WR9G078	
11. CONTROLLING OFFICE NAME AND ADDRESS Naval Postgraduate School Monterey, California 93940	12. REPORT DATE (11) June 1979	13. NUMBER OF PAGES 132
14. MONITORING AGENCY NAME & ADDRESS (if different from Controlling Office) (12) 134 P.	15. SECURITY CLASS. (of this report) Unclassified	16. DECLASSIFICATION/DOWNGRADING SCHEDULE
16. DISTRIBUTION STATEMENT (of this Report) Approved for public release; distribution unlimited.		
17. DISTRIBUTION STATEMENT (of the abstract entered in Block 20, if different from Report)		
18. SUPPLEMENTARY NOTES		
19. KEY WORDS (Continue on reverse side if necessary and identify by block number) Dropwise Condensation, Enhanced Heat Transfer, Condensers, Promoters, Coatings		
20. ABSTRACT (Continue on reverse side if necessary and identify by block number) → Three types of drop promoting coatings were applied to the outside of 15.9 mm (5/8 in) outside-diameter condenser tubes to determine their effect on heat transfer performance. The coatings included a new fluoroepoxy, a commercial series of fluorocarbon coatings, and sputtered TFE. Coating thickness varied from 0.02 to 12.7 microns. Steam at about 21 KPa (3 psia) was condensed on the outside surface of each coated tube, horizontally mounted in the		

UNCLASSIFIED

SECURITY CLASSIFICATION OF THIS PAGE(When Data Entered)

#20 - ABSTRACT - CONTINUED

center of a dummy tube bundle. Each test tube was cooled on the inside by water at velocities of 0.80 to 7.60 m/sec (3 to 25 ft/sec).

The overall heat transfer coefficient was determined directly from experimental data. The inside and outside heat transfer coefficients were determined by using the Wilson Plot technique.

Of the commercial fluorocarbon coatings, the "Nedox" coating on a copper-nickel tube enhanced the outside heat transfer coefficient by 53% and improved the corrected overall heat transfer coefficient by 27%. Of the sputtered TFE coated tubes, the 0.08-micron thick coating on a copper-nickel tube enhanced the outside heat transfer coefficient by 45% and improved the corrected overall heat transfer coefficient by 21%. Evidence of the effect of the thermal conductivity of the condensing surface substrate, and evidence of an optimum coating thickness were found.

UNCLASSIFIED

SECURITY CLASSIFICATION OF THIS PAGE(When Data Entered)

Approved for public release; distribution unlimited.

An Experimental Study of
Dropwise Condensation on
Horizontal Condenser Tubes

by

John Talbot Manvel, Jr.
Lieutenant, United States Navy
B.S.O.E., United States Naval Academy, 1972

Submitted in partial fulfillment of the
requirements for the degree of

MASTER OF SCIENCE IN MECHANICAL ENGINEERING

from the

NAVAL POSTGRADUATE SCHOOL

June 1979

Author

John Talbot Manvel Jr

Approved by:

J. J. Marto

Thesis Advisor

J. J. Marto

Chairman, Department of Mechanical Engineering

William M. Talles

Dean of Science and Engineering

ABSTRACT

Three types of drop promoting coatings were applied to the outside of 15.9 mm (5/8 in) outside-diameter condenser tubes to determine their effect on heat transfer performance. The coatings included a new fluoroepoxy, a commercial series of fluorocarbon coatings, and sputtered TFE. Coating thickness varied from 0.02 to 12.7 microns. Steam at about 21 KPa (3 psia) was condensed on the outside surface of each coated tube, horizontally mounted in the center of a dummy tube bundle. Each test tube was cooled on the inside by water at velocities of 0.80 to 7.60 m/sec (3 to 25 ft/sec).

The overall heat transfer coefficient was determined directly from experimental data. The inside and outside heat transfer coefficients were determined by using the Wilson Plot technique.

Of the commercial fluorocarbon coatings, the "Nedox" coating on a copper-nickel tube enhanced the outside heat transfer coefficient by 53% and improved the corrected overall heat transfer coefficient by 27%. Of the sputtered TFE coated tubes, the 0.08-micron thick coating on a copper-nickel tube enhanced the outside heat transfer coefficient by 45% and improved the corrected overall heat transfer coefficient by 21%. Evidence of the effect of the thermal conductivity of the condensing surface substrate, and evidence of an optimum coating thickness were found.

TABLE OF CONTENTS

I.	INTRODUCTION -----	14
	A. BACKGROUND INFORMATION -----	14
	B. PURPOSE OF STUDY -----	18
II.	EXPERIMENTAL FACILITY -----	19
	A. TEST FACILITY -----	19
	B. INSTRUMENTATION -----	20
	1. Flow Rate -----	20
	2. Pressure -----	21
	3. Temperature -----	21
	4. Data Collection and Display -----	21
	C. TEST TUBES -----	22
III.	EXPERIMENTAL PROCEDURES -----	26
	A. INSTALLATION AND PREPARATION OF CONDENSER TUBES -----	26
	B. SYSTEM OPERATION AND STEADY STATE CONDITIONS -----	27
	C. DATA REDUCTION PROCEDURES -----	27
	1. Overall Heat Transfer Coefficient -----	27
	2. Inside Heat Transfer Coefficient -----	29
	3. Outside Heat Transfer Coefficient -----	31
	4. Adjustments to T_{c_i} and T_{c_o} for Short Tubes -----	32
IV.	RESULTS AND DISCUSSION -----	35
	A. INTRODUCTION -----	35
	1. Performance of the Coatings -----	35
	2. Visualization of Dropwise Condensation -----	38

B.	CORRECTED OVERALL HEAT TRANSFER COEFFICIENTS --	39
C.	EFFECT OF TUBE WALL CONDUCTIVITY -----	41
D.	SIEDER-TATE COEFFICIENTS -----	41
E.	OUTSIDE HEAT TRANSFER COEFFICIENTS -----	43
F.	EFFECT OF COATING THICKNESS -----	44
V.	CONCLUSIONS -----	45
VI.	RECOMMENDATIONS -----	46
VII.	TABLES -----	48
VIII.	FIGURES -----	78
APPENDIX A:	OPERATING PROCEDURES -----	98
APPENDIX B:	SAMPLE CALCULATIONS -----	107
APPENDIX C:	UNCERTAINTY ANALYSIS -----	120
BIBLIOGRAPHY	-----	126
INITIAL DISTRIBUTION LIST	-----	129

LIST OF TABLES

Table I.	Designation of Stainless Steel Sheathed Copper Constantan Thermocouples -----	48
Table II.	Location of Teflon Coated Copper Constantan Thermocouples -----	49
Table III.	Summary of Coatings -----	50
Table IV.	Summary of Coated Tube Characteristics and Performance -----	51
Table V.	Raw Data for Uncoated (long) CuNi Tube. 3 Feb 79 -----	52
Table VI.	Raw Data for 12.7 μ m NRL Fluoroepoxy Coated CuNi Tube. 5 Feb 79. -----	53
Table VII.	Raw Data for 0.02 μ m NRL Fluoroepoxy Coated CuNi Tube. 8 Feb 79 -----	54
Table VIII.	Raw Data for 1.27 μ m NRL Fluoroepoxy Coated CuNi Tube. 9 Feb 79 -----	55
Table IX.	Raw Data for "Nedox" Coated CuNi Tube. 10 Feb 79 -----	56
Table X.	Raw Data for "Canadizing" Coated Ti Tube. 12 Feb 79 -----	57
Table XI.	Raw Data for "Tufрам" Coated Al Tube. 18 Feb 79 -----	58
Table XII.	Raw Data for 0.20 μ m Sputtered TFE Coated CuNi Tube. 19 Feb 79 -----	59
Table XIII.	Raw Data for 0.04 μ m Sputtered TFE Coated CuNi Tube. 22 Feb 79 -----	60
Table XIV.	Raw Data for 0.20 μ m Sputtered TFE Coated Ti Tube. 24 Feb 79 -----	61
Table XV.	Raw Data for 0.08 μ m Sputtered TFE Coated CuNi Tube. 26 Feb 79 -----	62
Table XVI.	Raw Data for 0.04 μ m Sputtered TFE Coated Ti Tube. 27 Feb 79 -----	63

Table XVII.	Raw Data for Uncoated (short) CuNi Tube. 28 Feb 79 -----	64
Table XVIII.	Results of Uncoated (long) CuNi Tube. 3 Feb 79 -----	65
Table XIX.	Results of 12.7 μ m NRL Fluoroepoxy Coated CuNi Tube. 5 Feb 79 -----	66
Table XX.	Results of 0.02 μ m NRL Fluoroepoxy Coated CuNi Tube. 8 Feb 79 -----	67
Table XXI.	Results of 1.27 μ m NRL Fluoroepoxy Coated CuNi Tube. 9 Feb 79 -----	68
Table XXII.	Results of "Nedox" Coated CuNi Tube. 10 Feb 79 -----	69
Table XXIII.	Results of "Canadizing" Coated Ti Tube. 12 Feb 79 -----	70
Table XXIV.	Results of "Tufрам" Coated Al Tube. 18 Feb 79 -----	71
Table XXV.	Results of 0.20 μ m Sputtered TFE Coated CuNi Tube. 19 Feb 79 -----	72
Table XXVI.	Results of 0.04 μ m Sputtered TFE Coated CuNi Tube. 22 Feb 79 -----	73
Table XXVII.	Results of 0.20 μ m Sputtered TFE Coated Ti Tube. 24 Feb 79 -----	74
Table XXVIII.	Results of 0.08 μ m Sputtered TFE Coated CuNi Tube. 26 Feb 79 -----	75
Table XXIX.	Results of 0.04 μ m Sputtered TFE Coated Ti Tube. 27 Feb 79 -----	76
Table XXX.	Results of Uncoated (short) CuNi Tube. 28 Feb 79 -----	77

LIST OF FIGURES

Figure 1.	Comparison of Path of Heat Conduction in Dropwise versus Filmwise Condensation ----	78
Figure 2.	Photograph of Test Facility -----	79
Figure 3.	Schematic Diagram of Steam System -----	80
Figure 4.	Test Condenser Schematic, Front View -----	81
Figure 5.	Test Condenser Schematic, Side View -----	82
Figure 6.	Diagram of Short Tube with Insulated Extensions Inside Test Condenser without Dummy Tubes -----	83
Figure 7.	Schematic Diagram of Cooling Water System ---	84
Figure 8.	Schematic Representation of Procedure Used to Find U_n -----	85
Figure 9.	Schematic Representation of Procedure Used to Find Sieder-Tate Parameter -----	86
Figure 10.	Schematic Representation of Procedure Used to Find Sieder-Tate Coefficients C_i , h_i and h_o -----	87
Figure 11.	Film Sequence of Dropwise Condensation -----	88
Figure 12.	Corrected Overall Heat Coefficient, U_c , versus Cooling Water Mass Flowrate for NRL Fluoroepoxy Coated Tubes -----	89
Figure 13.	Corrected Overall Heat Transfer Coefficient, U_c , versus Cooling Water Mass Flowrate for General Magnaplate Corporation Coated Tubes -	90
Figure 14.	Corrected Overall Heat Transfer Coefficient, U_c , versus Cooling Water Mass Flowrate for Sputtered TFE Coated CuNi Tubes -----	91
Figure 15.	Corrected Overall Heat Transfer Coefficient, U_c , versus Cooling Water Mass Flowrate for Sputtered TFE Coated Ti Tubes -----	92
Figure 16.	Wilson Plot for Uncoated CuNi (long) Tube ---	93
Figure 17.	Wilson Plot for "Nedox" Coated CuNi Tube ----	94

Figure 18.	Wilson Plot for Short 0.08 Sputtered TFE CuNi Tube -----	95
Figure 19.	Outside Heat Transfer Coefficient, h_o , versus Coating Thickness for NRL Fluroepoxy Coated CuNi Tubes -----	96
Figure 20.	Outside Heat Transfer Coefficient, h_o , versus Coating Thickness for Sputtered TFE Coated CuNi Tubes -----	97

NOMENCLATURE

A	- Area (m^2)
A _c	- Cross sectional area of test section (m^2)
c _p	- Specific heat ($\text{kJ/kg}^\circ\text{C}$)
D	- Diameter (m)
g _c	- Gravitational constant (kg m/N sec^2)
h	- Heat transfer coefficient ($\text{W/m}^2^\circ\text{C}$)
h _{fg}	- Latent heat of vaporization (W sec/kg)
ID	- Inside diameter (mm)
k	- Thermal conductivity ($\text{W/m}^\circ\text{C}$)
L	- Length of test tube (m)
LMTD	- Log mean temperature difference ($^\circ\text{C}$)
\dot{m}	- Mass flow rate of cooling water (kg/sec)
M	- Slope of Wilson Plot output from linear regression program
p	- Pressure (kPa)
pr	- Prandtl number = $\mu c_p / k$
pw	- Wetted perimeter (mm)
Q	- Heat flow rate (W/sec)
\dot{Q}	- Volumetric flow rate (l/m)
R	- Thermal resistance ($\text{m}^2^\circ\text{C/W}$)
Re	- Reynolds number = DG/μ
t	- Wall thickness (mm)
T	- Temperature ($^\circ\text{C}, ^\circ\text{K}$)
T _c	- Temperature of cooling water ($^\circ\text{C}$)

- U - Overall heat transfer coefficient ($\text{W/m}^2\text{°C}$)
- v - Water velocity (m/sec)
- V - Volume (m^3)
- Wp - Pumping power (kW)
- X - x axis input to linear regression program
- Y - y axis input to linear regression program

GREEK SYMBOLS

- Δ - Differential
- μ - Dynamic viscosity (kg/m hr)
- ρ - Fluid density (kg/m^3)

SI to English Conversions

- h - $1 \text{ W/m}^2\text{°C} = 0.1761 \text{ BTU/hr ft}^2\text{°F}$
- k - $1 \text{ W/m}^2\text{°C} = 0.5778 \text{ BTU/hr ft}^2\text{°F}$
- c_p - $1 \text{ kJ/kg}^{\circ}\text{C} = 0.23884 \text{ BTU/lbm}^{\circ}\text{F}$
- Q - $1 \text{ W/sec} = 9.4781 \times 10^{-4} \text{ BTU/sec}^2$
- μ - $1 \text{ kg/m hr} = 2419.2 \text{ lbm/ft hr}$
- ρ - $1 \text{ kg/m}^3 = 0.06243 \text{ lbm/ft}^3$
- p - $\text{pa} = 1.45038 \times 10^{-4} \text{ lbf/in}^2$
- T - $^{\circ}\text{C} = 5/9 (^{\circ}\text{F} - 32)$
 $^{\circ}\text{K} = 5/9 ^{\circ}\text{R}$
- L - $1 \text{ m} = 3.2808 \text{ ft}$
- A - $1 \text{ m}^2 = 10.7639 \text{ ft}^2$

ACKNOWLEDGMENT

The work presented here has been supported by the Naval Sea Systems Command, under the supervision of Mr. Charles Miller (Code 0331).

A special note of appreciation is extended to Ken Mothersell, Junior Dames and Tom Christian for their diligent technical assistance.

The assistance and cooperation of Dr. James Griffith of the Naval Research Laboratory is gratefully acknowledged.

I am especially thankful of the patient and competent guidance of Professor Paul J. Marto.

I. INTRODUCTION

A. BACKGROUND INFORMATION

As U. S. naval warships grow more sophisticated and complex, the need to reduce the size and weight of ship systems grows with them. On steam-powered warships, the propulsion plant dominates a large portion of the ship's overall weight and volume. Many of the components of the propulsion plant, the condenser among them, are under study to reduce their size and weight.

Naval condensers in use today are designed by heat transfer theory developed many years ago. Although such theory provides designs which are highly reliable, these designs are also oversized and bulky. Feasibility studies by Search [1] indicate that with the use of modern computer methods, using enhanced heat transfer techniques, size and weight of condensers may be reduced by as much as forty percent.

Dropwise condensation is one of the enhanced heat transfer techniques that may improve naval condensers. When a vapor condenses to a liquid on a cooled surface, it can condense in two ways: it can (1) wet the surface and form in a film, or (2) not wet the surface and form in discrete drops. A surface that does not become wet is called hydrophobic. The heat transfer advantage of dropwise condensation over filmwise condensation lies in the reduction

of the thermal resistance of the condensate. It is well-known that the thermal resistance to the conduction of heat is proportional to the length of the conduction path. In filmwise condensation, the conduction path of heat is through a relatively thick condensate layer, Figure 1(a). In dropwise condensation, the conduction path is shortened considerably because the heat is transferred through thousands of tiny drops rather than through a thick film, Figure 1(b). This results in an effective outside heat transfer coefficient which can be a factor of ten or more larger than those obtained with the filmwise mode.

The promotion of dropwise condensation can be accomplished in three ways: (1) by wiping the surface with a hydrophobic material, (2) by injecting hydrophobic material into the vapor and, (3) by permanently coating the condensing surface with a hydrophobic material. The first way is a laboratory technique and is of little value in naval condenser design. Injection of hydrophobic materials into the vapor has been successful in promoting dropwise condensation. However, injected promoter performances have been shown to be very sensitive to the vapor chemistry and impurities which degrade the promoter's hydrophobic character [2,3]. Furthermore, in terms of a naval steam plant, another additive in the already complex boiler feedwater chemistry problem is not desired. Thus, permanent promoters become the center of interest for naval steam condensers.

There are two types of permanent promoters: noble metals and organic polymers. Noble metals have been the subject of extensive studies by Erb and Thelen of the Franklin Institute [4]. They promoted dropwise condensation of water vapor on gold, palladium, and rhodium for over 10,000 hours (1.14 years), and concluded that it was economically feasible to use gold plated coatings in large saltwater conversion plants. However, Wilkins, Bromley, and Read [5] found conflicting results using noble metals, and concluded that gold, the best promoter Erb and Thelen found, does not permanently promote dropwise condensation. They attributed Erb and Thelen's results to some organic contamination. Add this conflicting data to the ever increasing prices of noble metals, especially gold, and the use of noble metals becomes less attractive.

Organic polymers have well-known hydrophobic qualities. However, they also have low thermal conductivities making them poor conductors of heat. Early studies using organic polymers in relatively thick coatings reflected the poor conductivity of the organic polymer. Smith [6] sprayed Teflon on 15.9 mm OD copper-nickel tubes and found little improvement in the overall heat transfer coefficient. Cox [7] found that Teflon coatings, 12.7 microns (0.5 mils) thick, promoted dropwise condensation and improved the overall heat transfer coefficient by 22%. Coated condenser tubes have also been studied at NSRDC Annapolis, Maryland [8].

Tubes covered with a 12.7 micron (0.5 mils) thick coating of Teflon were found to have only a 10% improvement in the overall heat transfer coefficient. It was also found that Teflon coated surfaces were rendered ineffective by contamination from rust, salt, etc.

Results were more encouraging when the thickness of the coating was decreased. Depew and Reisberg [9] used a Teflon coating 6.35 microns (0.25 mils) thick on aluminum tubes and found improvements in heat transfer rates as much as 40 to 100%. Erb and Thelen [10] pointed the way to the use of ultra-thin coatings. Using a vapor deposition process developed by Union Carbide, they experimented with vapor-deposited polymers, hexafluorobenzene and paraxylylene. Although the hexafluorobenzene did not work, paraxylylene at thicknesses of 0.25 micron (0.01 mil) and 1 micron (0.04 mil) on chromium plated copper-nickel surfaces did promote dropwise condensation. They concluded that ultra-thin polymer coatings appear to be profitable areas for study. More recently, Tanasawa [11] emphasized the use of ultra-thin coatings, and cited that with the rapid advance in materials technology and in coating processes, particularly glow discharge and electrophoresis, the promise of a permanent polymer promoter is not too far away.

A report by Croix and Legois [17] using gold as the promoter hints of potentially significant benefits of dropwise condensation in tube banks. They found that, contrary

to filmwise data, for a bundle at least 16 tubes in depth, there was no attenuation of the performance of the tubes situated lower in the tube bundle when compared to the tubes near the top. The prospect of not only increasing a single tube's heat transfer performance using a permanent drop promoter, but also increasing the performance of an entire tube bundle provides the motivation to look at new coatings and new techniques of applying coatings to find a permanent promoter that will work.

B. PURPOSE OF STUDY

The purpose of this study was twofold:

- (1) to test new organic polymer coatings and new coating techniques that have not yet been applied to the study of dropwise condensation, and
- (2) to obtain heat transfer data and determine the effect of coating thickness.

The new coatings selected for study were a "C-6" fluoro-epoxy coating developed by the Chemistry Division of the Naval Research Laboratory, and commercial coatings developed by the General Magnaplate Corporation: "Nedox," "Canadizing," and "Tufram." These coatings were selected on the basis of their advertised qualities of durability and hydrophobicity.

The coating technique selected for study was sputtering. Sputtering is a deposition process widely used in the electronic industry for applying ultra-thin coatings to semiconductors.

II. EXPERIMENTAL FACILITY

A. TEST FACILITY

The test facility, Figure 2, was designed by Beck [13] and built and tested by Pence [14]. Using this facility, Fenner [15] has conducted tests on geometrically enhanced condenser tubes.

The test facility consists of an electrically powered boiler that produces 45.4 kg/hr (100 lbm/hr) of saturated steam. The steam passes through a steam separator, a throttle valve, and a desuperheater before it enters the condenser; Figures 3, 4, and 5. Pressure in the condenser is maintained at 155 mm Hg (3 psia) by a vacuum pump.

The condenser consists of nine 15.9 mm, 18 gauge 90-10 copper-nickel tubes arranged in a typical condenser configuration with a spacing-to-diameter ratio (S/D) of 1.5. The center tube is the only one with cooling water passing through it. Steam condenses on the 91.44 cm length of this test tube or flows through to a secondary condenser. Condensate is collected in a hotwell and is pumped to a feedwater reservoir tank before returning to the boiler as needed.

Cooling water for the test tube is pumped from a supply tank through an 18.8 gpm rotameter. After passing through the test tube, the water is returned to the supply tank via a dry cooling tower. A detailed description of the

components used in the test facility may be found in Pence [14] and Reilly [16].

Two modifications were made to the condenser for this study. First, the condenser window frame was modified (Figure 4) because excessive non-uniform thermal expansion during operation kept breaking the glass viewing windows. Two braces were therefore inserted, and the o-ring groove was modified to accommodate three 23 cm (9 in) long viewing windows in the window frame. The second modification occurred when using the test tubes which were coated with sputtered Teflon. Because of the size of the deposition chamber in which these tubes were coated, they could only be 152.4 mm (6 in) long. These shortened tubes were therefore attached by epoxy to insulated tube extensions so they could be placed in the center of the condenser, as shown in Figure 6.

B. INSTRUMENTATION

1. Flow Rate

Fulton rotameters were used to measure the flow rate of water in the cooling water system and the desuperheater. They were calibrated previously by Reilly [16]. Their accuracy was checked by recording pressure drops at ten percent increments of flow through a standard 90-10 copper-nickel 15.9 mm (0.625 in) OD tube and comparing the pressure drops with previous runs on the standard copper-nickel tube. Recorded pressure drops deviated from previously recorded pressure drops by no more than one percent.

2. Pressure

Several different types of pressure measurement devices were used in this facility. They were: a Bourdon tube pressure gauge which was used to measure boiler pressure, a compound gauge which was used to measure the secondary condenser pressure, an absolute pressure transducer and a 760 mm mercury manometer which were used to measure the test condenser pressure, and a 3.6 m mercury manometer which was used to measure the cooling water pressure drop across the test tube [15].

3. Temperature

There were three types of thermocouples used in this facility. Stainless steel sheathed, copper-constantan thermocouples were used as the primary temperature monitoring devices. Table I lists the locations monitored. Figure 3 shows the location of six vapor-space thermocouples. Cooling water thermocouples were located as shown in Figure 7. Teflon-coated copper-constantan thermocouples were used as secondary measuring devices. Table II lists the locations monitored using these thermocouples. An iron-constantan thermocouple was used to measure the boiler temperature [15].

4. Data Collection and Display

An autodata collection system was utilized to record and display the temperatures in degrees Celsius obtained from the primary thermocouples and to record and display the pressure in cm Hg inside the test condenser. See Table I for channel numbers of the temperature monitoring devices.

A 28-channel digital pyrometer was utilized to display the temperatures obtained from the secondary thermocouples and a single channel pyrometer displayed the temperatures from the iron-constantan thermocouple. See Table II for channel numbers.

C. TEST TUBES

Three sets of test tubes were used in this study. The first set consisted of six 1.22 m (48 in) long, 15.9 mm (0.625 in) OD, 18 gauge 90-10 copper-nickel tubes coated on the outside with a fluoroepoxy by Dr. James Griffith of the Naval Research Laboratory's Chemistry Division. Each tube was coated with a different thickness as shown in Table III. The tubes were coated using the following procedure [17]. The tubes were first cleaned using water, detergent, and a "Scotch-Brite" abrasive pad, and then were thoroughly rinsed with water. A dipping apparatus was set up which consisted of a 19 mm (0.75 in) I.D. vertical tube capped on the lower end, and a pulley arrangement to withdraw the tubes manually at a rate of 153 mm/sec (6 in/sec). The resin employed was NRL "C-6" fluoroepoxy with an equivalent amount of Si-2 silicone amine as the curing agent. The solvent was Freon TF into which the resin and curing agent were dissolved at 10% by weight.

The thickness of the 2.54 micron (0.1 mil) film was determined by measuring the coating thickness on a flat sample dipped in the solution by an Elcotector MK III

General Purpose Eddy Current Comparator. The thickness of the 12.7 micron (0.5 mil) film was presumed to be achieved by dipping a tube into the proven solution five times. The solution was then diluted 9/1 with Freon TF for dipping to achieve a presumed thickness of 0.254 micron (0.01 mil). Multiple dipping was again repeated in this solution to achieve the presumed coating thickness of 1.27 micron (0.05 mil). The solution was again diluted 9/1 with Freon TF for dipping to achieve the presumed thickness 0.0254 micron (0.001 mil), and again the multiple dipping procedure was repeated to achieve the presumed coating thickness of 0.127 micron (0.005 mil). Unfortunately, the last two coatings appeared to be discontinuous. The coatings were allowed to dry and pre-cure at room temperature for three days before being cured in an oven at 60°C for one hour followed by 120°C for three hours [17].

The second set of tubes consisted of three 1.22 m (48 in) long tubes coated on the outside by the General Magnaplate Corporation (GMP). A 15.9 mm (0.675 in) OD, 18 gauge, 90-10 copper-nickel tube was coated with GMP's "Nedox" coating. "Nedox" is a proprietary process of GMP in which a hard surface of nickel alloy is deposited on a copper-nickel surface. The structure of the deposit is extremely porous, and a series of proprietary processes enlarge the micro-pores to accept controlled infusion of polytetra fluorethylene (Teflon) [18]. The Nedox coating

was 12.7 micron (0.5 mil) thick. A 15.9 mm (0.625 in) OD, 14 gauge, aluminum tube was coated with GMP's "Tufram" coating. "Tufram" is a patented, proprietary anodizing process that converts the aluminum surface to aluminum oxide (Al_2O_3) and replaces the H_2O of the newly formed ceramic surface with TFE. This results in a continuous, lubricating plastic-ceramic surface of which TFE particles become an integral part [19]. The third tube, a 15.9 mm (0.625 in) OD, 22 gauge, titanium tube, was coated with GMP's "Canadizing" coating. "Canadizing" is a recently perfected electro-chemical process which produces a surface with controlled porosity into which TFE penetrates thoroughly [20].

The third set of tubes consisted of six 152.4 mm (6 in) long tubes specially coated with Teflon by the vacuum deposition "S-Gun" sputtering process of the Palo Alto Vacuum Division of Varian Associates. Three 15.9 mm (0.625 in) OD, 18 gauge, 90-10 copper-nickel tubes and three 15.9 mm (0.625 in) OD, 22 gauge titanium tubes were sputtered with three coatings of Teflon: .04 micron, .08 micron, and 0.20 micron thick.

Two uncoated 15.9 mm (0.625 in) OD, 18 gauge, 90-10 copper-nickel tubes were tested in filmwise condensation to be used as a basis for comparison. One tube was a standard 1.22 m (48 in) long tube; the second was a 152.4 mm (6 in) long tube to be used in comparison with the short, sputtered coated tubes. Tube preparation procedures outlined in Pence

(14] were followed to insure that filmwise condensation occurred on the uncoated tubes.

III. EXPERIMENTAL PROCEDURES

A. INSTALLATION AND PREPARATION OF CONDENSER TUBES

A thermocouple was installed on each tube to measure wall temperature. A 100 mm long groove, 0.5 mm deep, was machined axially in the center of the tube on the outside surface. The thermocouple was then attached in the groove with fast-setting epoxy. Care was taken to insure that coatings on the tubes were not disturbed. The two uncoated copper-nickel tubes were prepared in accordance with the procedure given in Pence [14] to insure filmwise condensation.

The short (15.24 cm) titanium and copper-nickel tubes coated with sputtered TFE required special preparation for testing. Since the normal tube length for the condenser was 1.22 m, these short tubes were installed by the following method. Prior to a run, the test tube to be run was attached to two 0.54 m long stainless steel extensions to make up a 1.22 m long test tube (Figure 6). The front window frame and windows were removed from the condenser as were several dummy tubes to permit easy access to the test tube during installation. The test tube was then inserted horizontally into the condenser insuring that the sputtered TFE coated portion was in the center with the attached wall thermocouple facing down. The stainless steel tubing extensions were then insulated with flexible acrylic tubing, 4.76 mm thick, Figure 6. The dummy tubes were then reinstalled in

the tube bundle, and the condenser was closed up, ready for use. The same procedure was used for the titanium tubes coated with sputtered TFE except that titanium extensions were used.

B. SYSTEM OPERATION AND STEADY STATE CONDITIONS

Pence [14] and Reilly [16] wrote a detailed set of operating procedures for this system. Light-off procedures were modified to clarify the valve positions. These procedures are included in this report as Appendix A.

Operation of the system was accomplished in general agreement with system operation outlined in Pence [14]. Minor modifications were made for the convenience of the operator.

C. DATA REDUCTION PROCEDURES

In evaluating the data from the runs, it was decided to present the data in such a way as to make it immediately useful to the designer.

Appendix B, the sample calculations, is a complete listing of equations used to evaluate the data. Appendix C is the uncertainty analysis used to determine the probable error in the data reduction equations, followed by a sample uncertainty analysis for the 0.08 μ m sputtered TFE copper-nickel tube.

1. Overall Heat Transfer Coefficient

The method employed to arrive at the overall heat transfer coefficient is straightforward and similar to that employed by many researchers in the past.

The heat transfer rates to the cooling water is given by

$$Q = \dot{m} c_p (T_{c_o} - T_{c_i}) \quad (1)$$

The heat transfer rate can also be found from the overall heat transfer coefficient by

$$Q = U_N A_N \text{LMTD} \quad (2)$$

where

$$\text{LMTD} = \frac{(T_v - T_{c_i}) - (T_v - T_{c_o})}{\ln \left[\frac{T_v - T_{c_i}}{T_v - T_{c_o}} \right]} \quad (3)$$

Combining equations (1), (2) and (3), it is found that

$$U_N = \frac{\dot{m} c_p}{A_N} \ln \left[\frac{T_v - T_{c_i}}{T_v - T_{c_o}} \right] \quad (4)$$

An illustration of the procedures to arrive at U_N is given in Figure 8.

To remove the effect of the tube wall material, a corrected overall heat transfer coefficient is found from

$$U_C = \frac{1}{\frac{1}{U_N} - R_w} \quad (5)$$

where R_w is the calculated wall resistance

2. Inside Heat Transfer Coefficient

The Nusselt number on the inside is found from the Sieder Tate relationship, as [21]:

$$N_u = \frac{h_i D_i}{k_b} = C_i Re^{0.8} Pr^{1/3} (\mu/\mu_w)^{0.14} \quad (6)$$

With this well-known correlation, all fluid properties are evaluated at the average bulk temperature of the cooling water. The effect of the wall temperature is only felt by a viscosity ratio $(\mu/\mu_w)^{0.14}$. In equation (6), C_i is referred to as the Sieder Tate coefficient which is normally expressed as between 0.023 - 0.027 for smooth tubes. The remainder of the right hand side of the above equation $(Re^{0.8} Pr^{1/3} (\mu/\mu_w)^{0.14})$ is referred to as the Sieder Tate parameter, and the procedure for arriving at this value is illustrated schematically in Figure 9. The Wilson plot is used to arrive at the value of the Sieder Tate coefficient. The Wilson plot was developed in 1915 [22] and has since been modified by several researchers. The procedure used in this research was developed by Briggs and Young [23].

The Wilson plot is a plot of $1/U_N$ versus the inverse of the Sieder Tate parameter which should be a straight line

when varying the cooling water velocity. The reasoning behind the Wilson plot can be seen in the following development.

For smooth tubes, the overall heat transfer coefficient can be written as:

$$U_N = \frac{1}{\frac{D_o}{D_i h_i} + R_w + \frac{1}{h_o}} \quad (7)$$

or,

$$\frac{1}{U_N} = \frac{D_o}{D_i h_i} + R_w + \frac{1}{h_o} \quad (8)$$

If $(R_w + \frac{1}{h_o})$ is assumed to be constant, and equation (6) is solved for h_i in terms of the Sieder Tate parameter, equation (8) can be rewritten as

$$\frac{1}{U_N} = \frac{D_o}{C_i k_b} \text{Re}^{-0.8} \text{Pr}^{-1/3} (u/u_w)^{-0.14} + B \quad (9)$$

where

$$B = R_w + \frac{1}{h_o} = \text{constant}.$$

The form of equation (9) is then exactly that of a straight line,

$$Y = MX + B \quad (10)$$

where:

$$Y = \frac{1}{U_N} \quad (10a)$$

$$X = \frac{1}{\text{Sieder Tate parameter}}, \text{ and} \quad (10b)$$

$$M = \frac{D_o}{C_i K_b} \quad (10c)$$

The values of $1/U_N$ and the Sieder Tate parameter are obtained by varying the water velocity and holding the other parameters, such as water temperatures, steam vapor temperatures and condenser tube wall temperature, nearly constant. When $1/U_N$ is plotted versus $Re^{-0.8} Pr^{-1/3} (u/u_w)^{-0.14}$ a linear regression subroutine [14] fits these points to a straight line and then solves for the slope, M , and the intercept, B . Knowing the slope, M , the Sieder Tate coefficient C_i can be found from equation (10c). The inside heat transfer coefficient, h_i , is then found from equation (6).

The cooling water properties (p, u, K, c_p and Pr) at the bulk temperature were solved for as shown in Appendix B. Appendix B also demonstrates the procedure for arriving at the water viscosity evaluated at the condenser tube wall temperature, u_w .

3. Outside Heat Transfer Coefficient

The outside heat transfer coefficient, h_o , can be found from equation (7) knowing U_N , h_i , and R_w . Figure 10 schematically illustrates the various steps outlined above.

4. Adjustments to T_{c_i} and T_{c_o} for Short Tubes

As mentioned earlier, the sputtered TFE tubes could only be 152 mm long. To test them in the test condenser, they were attached to insulated tube extensions, Figure 6. However, the temperature measurements of the cooling water inlet temperature, T_{c_i} , and the cooling water outlet temperature, T_{c_o} , were set up for a full size tube, 1.22 m long. Because of the large temperature difference between the steam vapor and the cooling water, and because of a 5 to 1 surface area ratio between the insulated tube extensions and the short test tube, heating of the cooling water through the insulation was not negligible. A closer examination of the insulated extensions in the condenser also revealed an axial gap between the insulation and tube sheet where filmwise condensation was occurring. This further contributed to the erroneous heating of the cooling water. Therefore, for the short tube, T_{c_i} was higher than actually measured, and T_{c_o} was lower than actually measured. Since the heat transfer data depends on an accurate measurement of T_{c_i} and T_{c_o} , the following method was used to correct for T_{c_i} and T_{c_o} .

The measured heat transfer rate

$$Q_m = \dot{m} c_p (T_{c_o} - T_{c_i}) \quad (11)$$

can be considered to be made up of three terms:

$$Q_m = Q_{CORR} + Q_{INS} + Q_{GAP} \quad (12)$$

where

Q_{CORR} = the correct heat transfer rate through the test tube

Q_{INS} = the heat transfer rate through the insulation

Q_{GAP} = the heat transfer rate through the gap between the insulation and tube sheet.

Therefore,

$$Q_{CORR} = Q_m - (Q_{INS} + Q_{GAP}) \quad (13)$$

and the correct heat transfer rate for the short test tube can be considered to be:

$$Q_{CORR} = \dot{m} C_p \Delta T_{CORR} \quad (14)$$

Solving for the correct temperature difference across the short test tube

$$\Delta T_{CORR} = \frac{Q_{CORR}}{\dot{m} C_p} \quad (15)$$

which can be compared to the measured temperature difference

$$\Delta T_m = (T_{c_o} - T_{c_i}) , \quad (16)$$

the temperature adjustment is then

$$T_{adj} = \frac{\Delta T_m - \Delta T_{CORR}}{2} \quad (17)$$

The measured cooling water inlet temperature, T_{c_i} , was then corrected to obtain an inlet temperature for the short tube, $T_{c_i}^*$

$$T_{c_i}^* = T_{c_i} + T_{adj} , \quad (18)$$

and an outlet cooling water temperature for the short tube, $T_{c_o}^*$, was calculated as:

$$T_{c_o}^* = T_{c_o} - T_{adj} . \quad (19)$$

Appendix B contains a complete listing of the equations used to calculate the temperature adjustment. Included is a sample calculation for the 0.08 μm sputtered TFE copper-nickel tube.

IV. RESULTS AND DISCUSSION

A. INTRODUCTION

Table IV lists the various tubes which were tested with their corresponding characteristics together with selected heat transfer data. Tables V through XVII list the raw data obtained from the experiments, and Tables XVIII through XXIX list all the computed data used to derive the tube performance.

Tube X, the uncoated full length (1.22 m) 90-10 copper-nickel tube, was used for several preliminary runs to ascertain that the system was operating normally. Once that was assured, Tube X was prepared according to procedures to insure filmwise condensation and then tested. This data then became the standard from which all the full length coated tubes were compared. A similar short tube, Tube Z, was used as the standard for the short coated tubes.

1. Performance of the Coatings

The first set of tubes tested after Tube X were the 90-10 copper-nickel tubes coated with the NRL fluoro-epoxy. Tube A, with the 12.7 micron thick coating, was tested first. It promoted dropwise condensation throughout the four hour data run. Enthusiasm over its drop-promoting performance subsided the following morning when the tube was removed from the condenser. Large discolored patches covered the top of the tube where the steam directly impinged.

In addition, streaked drops of re-solidified epoxy covered the underside of the tube. Obviously, the fluoroepoxy had dissolved. Tests on the fluoroepoxy continued in hopes that the coating's dissolution would not occur again. Tube F, whose initial coating was discontinuous and 0.02 micron thick, was next tested. It did not promote dropwise condensation at all. Tube C, the 1.27 micron thick coating was next tested. Dropwise condensation occurred initially on the tube, but within two hours after the start of condensation, dropwise was occurring only on the underside of the tube, while filmwise was occurring on the top and sides of the tube. Inspection after removal, revealed discolored patches in the coating on the top of the tube, similar to Tube A. Since it was clear that the fluoroepoxy coating was dissolving, no further tests on the fluoroepoxy coated tubes were conducted.

The General Magnaplate Corporation coatints were next tested. Tube G, the "Nedox" coated copper-nickel tube, vigorously promoted dropwise condensation throughout the four hour data run. Tube G was also photographed using 16 mm movie film, and it vigorously promoted dropwise condensation throughout the film session with no fading or discoloring of the coating. This was not true of the "Tufam" or "Canadizing" coated tubes. "Canadizing" did promote dropwise condensation initially, but the mode of condensation faded to a mixed mode (both dropwise and filmwise) of

condensation on the top of the tube, while dropwise condensation continued on the underside. Inspection of Tube H after the run showed that the "Canadizing" coating had faded on top. When sprinkled with water, the faded sections became wet, while the underside promoted droplets. Tube I, the "Tufram" coated tube, initially exhibited the same pattern of condensation, dropwise at first then fading to a mixed mode on top. However, after two hours of condensation, the mode of condensation was almost completely filmwise over the entire length and circumference of the tube. Inspection after removal from the condenser showed that the coating faded in streaks circumferentially around the tube. When sprinkled with water, the coating became completely wet, exhibiting none of its previous hydrophobic character.

An explanation of why "Nedox" performed well, while "Canadizing" and "Tufram" did not, may lie with the respective sublayers of the coatings. The "Nedox" process places a layer of nickel on the tube into which TFE is infused, while "Tufram" and "Canadizing" processes form a porous oxide on the tube surface into which TFE is infused. It is well documented in the literature that the presence of an oxide on the condensing surface degrades the drop promoting characteristic of the surface [2,4,25]. Since the coatings were of minimum thickness, the infused TFE layer was probably not thick enough to inhibit the degrading effect of the oxide sublayer.

After all of the full-sized tubes were tested, the short sputtered TFE coated tubes were tested. In general, all the sputtered TFE coated tubes vigorously promoted dropwise condensation. However, all the coatings showed a general fading after testing. When sprinkled with water after testing, all the coatings still showed a hydrophobic character of non-wetting.

When the raw data from the short tubes were first reduced, heating through the insulation was assumed to be insignificant. This resulted in outside heat transfer coefficients 25% higher than the outside heat transfer coefficient of the best performing full size tube, tube G - the "Nedox" coated tube. The assumption of no heating through the insulation became suspect. When the data from the short uncoated tube was reduced and the outside heat transfer coefficient for filmwise condensation remained at the same order of magnitude as the outside heat transfer coefficients during dropwise, the suspicions were confirmed. A temperature subroutine, TADJ, as discussed before in Chapter III.C.4, was therefore added to compensate for the heating of the cooling water through the insulated extensions. The testing of the short tubes concluded the experimental data runs.

2. Visualization of Dropwise Condensation

Figure 11 is a sequence of six frames taken from the movies obtained during dropwise condensation on Tube G,

the "Nedox" coated tube. In the first frame, the arrow points to a large drop of condensate which is about to roll off the top of the tube. The second frame, 0.10 seconds later, captures the drop rolling down the tube and sweeping its path clear of condensate. The third frame, 0.06 seconds later, shows the drop leaving the tube and the swept path behind it. In the fourth frame, 0.08 seconds later, tiny drops can just be seen forming in the swept path. In the next two frames, the new drops can be seen growing to a point where they are ready to roll off. The sequence of six frames covered 1.06 seconds. This sequence illustrates the cyclic nature of dropwise condensation.

B. CORRECTED OVERALL HEAT TRANSFER COEFFICIENTS

Figures 12 through 15 compare the corrected overall heat transfer coefficients for the coated tubes to the uncoated tube. Table IV lists the U_C ratio of the coated tubes to the uncoated tube at a specific cooling water velocity of 3 m/s.

As seen in Figure 12, for the NRL coated tubes, only the tube with the 1.27 micron thick coating produced a superior U_C than the uncoated tube. A 24% improvement occurred at a flowrate of 0.42 kg/sec (3 m/s). This 24% improvement, however, occurred while the mode of condensation was changing from dropwise to a mixed mode because the coating was dissolving.

Of the tubes coated with the GMP coatings, as seen in Figure 13, the "Nedox" coated tube had a 28% increase in U_C at 0.42 kg/sec (3 m/s), and the "Canadizing" coated titanium tube had a 12% increase in U_C at 0.52 kg/sec (3 m/s). The "Tufram" coated aluminum tube had a 14% decrease in U_C at 0.42 kg/sec (3 m/s). If the order of performance is compared to the coating thickness, the heat transfer performance varies inversely with the coating thickness. "Nedox" with a coating thickness of 5.0 microns produced the best U_C , while "Tufram" with a coating thickness of 10.0 microns, produced the worst U_C among the three. Moreover, "Nedox" has a sublayer of nickel which is a good conductor of heat, while "Canadizing" and "Tufram" have oxide sublayers which are poor conductors of heat. Thus, coating thickness and sublayer material influenced the corrected overall heat transfer coefficient results.

Of the short 90-10 copper-nickel tubes coated with sputtered TFE, as seen in Figure 14, the 0.08 micron thick coating produced a 21% improvement in U_C , and the 0.04 micron thick coating produced an 8% improvement in U_C at 0.42 kg/sec (3 m/s). As with the NRL fluoroepoxy coated tubes, the coating with an intermediate thickness was noted to produce the best performance. This will be elaborated on later in the discussion.

Of the short titanium tubes coated with sputtered TFE, it can be seen in Figure 15 that neither tube showed an improved performance during dropwise condensation.

C. EFFECT OF TUBE WALL CONDUCTIVITY

The only difference between the short copper-nickel and titanium tubes was their respective thermal conductivities. The tubes were identically prepared, and they both experienced excellent dropwise condensation. Yet their heat transfer performance, in terms of the corrected overall heat transfer coefficient, were markedly different. Since the sputtered coating was the same on each tube, this result suggests that the conductivity of the condensing surface substrate, i.e., the tube wall, influences the rate of heat transfer in dropwise condensation. In the literature, there are two opposing views concerning the effect of the wall thermal conductivity on dropwise condensation. Rose [26] has obtained experimental data to support his contention that low thermal conductivity of the condensing surface substrate does not affect the rate of heat transfer in dropwise condensation. On the other hand, Mikic [27] also has experimental data to support the opposite view that low thermal conductivity does reduce the rate of heat transfer in dropwise condensation. Results of this report provide more evidence that the thermal conductivity does affect the heat transfer rate in dropwise condensation.

D. SIEDER-TATE COEFFICIENTS

As seen in Table IV, the Sieder-Tate coefficient for all the full length tubes was 0.1026 ± 0.002 , which is nearly the same as those reported by Reilly [16] and Fenner [15]

for smooth tubes, and is between the normally quoted values of 0.023 to 0.027. Figure 16 shows the Wilson Plot for the uncoated full length copper-nickel tube. The solid line is obtained from the linear regression subroutine which fits the data of this report. Figure 17 is the Wilson Plot for the "Nedox" coated tube. The dashed line was generated by Fenner [15] for his smooth tube. It can be seen from the two graphs that the results agree reasonably with those of Fenner [15]. The differences reflect minor variations in the bulk properties of the cooling water.

For the short tubes, as seen in Table IV, the Sieder-Tate coefficient was 0.029 ± 0.003 . In this case of a fully developed cooling water velocity profile, the inside heat transfer coefficient is highest at the beginning of the test section where the temperature difference is the largest, and then decreases to a minimum value as the length increases to the limit. In the case of the short tubes, the short length of the test tube prevents the inside heat transfer coefficient from approaching the minimum value. Consequently, a larger average inside heat transfer coefficient and Sieder-Tate coefficient results.

Figure 18 is a Wilson Plot of the short, 0.08 micron sputtered TFE coated copper-nickel tube. The solid line is obtained from the linear regression subroutine to fit the data and the dashed line is from Fenner [15]. The smaller slope of the short tube reflects the larger Sieder-Tate

coefficient mentioned above. Although the two lines show reasonable agreement, the scattering of the data points along the solid line reflects the greater uncertainty associated with the data of the short tubes due to the corrections made on the cooling water temperatures, as mentioned in Chapter III.

E. OUTSIDE HEAT TRANSFER COEFFICIENT

Table IV lists the average outside heat transfer coefficients with their standard deviations for all of the tested tubes, and also the ratios of the outside heat transfer coefficients for the coated and the uncoated tubes. The "Nedox" coated tube was the full length tube with the best outside heat transfer coefficient, having a 53% enhancement. Also the 1.27 micron fluoroepoxy coated tube had a 41% enhancement and the "Canadizing" coated tube showed a 31% enhancement of the outside heat transfer coefficient, even though the mode of condensation was changing from a dropwise to a mixed mode during their respective runs.

Of the short tubes coated with sputtered TFE, only the copper-nickel tubes showed an enhancement of the outside heat transfer coefficient. Tube K, with a 0.08 micron thick coating, had a 45% enhancement of the outside heat transfer coefficient, and tube L, with a 0.04 micron thick coating, had a 35% enhancement.

F. COATING THICKNESS

If the data from the fluoroepoxy coated copper-nickel tubes are compared with the data of the sputtered TFE coated copper-nickel tubes, it can be seen that for each type of coating, the coating of intermediate thickness provided the best enhancement. Figures 19 and 20 compare the outside heat transfer coefficient versus coating thickness for the fluoroepoxy and sputtered TFE coated copper-nickel tubes respectively. These figures illustrate the superior outside heat transfer coefficient at the intermediate coating thickness. The data suggests that there is an optimum thickness for an organic polymer where the coating is thick enough to promote dropwise condensation, yet thin enough to provide a low thermal conduction resistance.

V. CONCLUSIONS

1. For the full length tubes, the best performance was obtained by the "Nedox" coated copper-nickel tube which had an outside heat transfer coefficient 1.53 times greater than the value for the uncoated tube. This resulted in a 27% enhancement of the corrected overall heat transfer coefficient.

2. For the short tubes, the best results were obtained by the 0.08 micron sputtered TFE coated copper-nickel tube which had an outside heat transfer coefficient 1.45 times the value of the uncoated tube. This resulted in a 21% enhancement of the corrected overall heat transfer coefficient.

3. Evidence of the effect of the thermal conductivity of the condensing surface substrate (tube wall) on dropwise condensation was found. Dropwise condensation enhanced the heat transfer performance of the sputtered TFE coated copper-nickel tubes, but did not enhance the heat transfer performance of the sputtered TFE coated titanium tubes.

4. Evidence of the effect of coating thickness on dropwise condensation was found. The data showed that an optimum coating thickness may exist.

VI. RECOMMENDATIONS

From the results of this experiment, several questions can be asked. To stimulate continued use of the test facility, the following recommendations are made.

1. Determine why the NRL fluoroepoxy dissolved.
2. Determine the possibility of reducing the coating thickness of "Nedox" and, if possible, test tubes with reduced coatings of "Nedox."
3. Conduct long-term tests on "Nedox" and sputtered TFE coated tubes to determine the long term durability of these coatings to condensing steam.
4. Conduct tests on coated tubes in a tube bundle to determine the effect of condensate inundation on dropwise condensation.
5. Continue studying the effect of coating thickness of organic polymers on dropwise condensation.
6. Continue studying the effect of wall thermal conductivity on heat transfer performance during dropwise condensation.
7. Examine the surface chemistry of sputtered TFE on various metals using the Scanning Electron Microscope, and in conjunction with heat transfer tests, determine the effect of surface chemistry variations on heat transfer performance.

8. Determine the possibility of coating full size tubes by sputtering to obtain more comparable heat transfer data with full size coated tubes.

9. Exploit the sputtering process to test multiple-layered coatings of different materials for the promotion of dropwise condensation.

VII. TABLES

Channel Number	Designation*	Channel Number	Designation*
40	Tc _i	47	T _v
41	Tc _o	48	T _v
42	Tc _o	49	T _v
43	Tc _o	50	T _v
44	Tc _o	51	T _w
45	T _v	52	Hotwell
46	T _v		

* See Figures 3 and 7 for locations.

Table I. Designation of Stainless Steel Sheathed
Copper Constantan Thermocouples

Channel Number	Location	Channel Number	Location
1	Hot Well	6	Condensate Header
2	Feedwater Tank	7	Tc into Cooling Tower
3	Condenser Window	8	Tc out of Cooling Tower
4	T_{c_i}	9	Cooling Tower Ambient
5	T_{c_o}		

Table II. Location of Teflon Coated Copper
Constantan Thermocouples

Tube	Material	Tube wall thickness mm	Coating	Coating thickness μm
------	----------	------------------------------	---------	----------------------------

LONG TUBES (122 cm)

A	CuNi	1.27	NRL Fluoroepoxy	12.70
B	CuNi	1.27	NRL Fluoroepoxy	2.54
C	CuNi	1.27	NRL Fluoroepoxy	1.27
D	CuNi	1.27	NRL Fluoroepoxy	0.25
E	CuNi	1.27	NRL Fluoroepoxy	0.13*
F	CuNi	1.27	NRL Fluoroepoxy	0.02*
G	CuNi	1.270	Nedox	5.0 ± 2.5
H	Ti	0.560	Canadizing	7.5 ± 2.5
I	Al	2.540	Tufram	10.0 ± 7.5

SHORT TUBES (15.24 cm)

J	CuNi	1.27	Sputtered TFE	0.04
K	CuNi	1.27	Sputtered TFE	0.08
L	CuNi	1.27	Sputtered TFE	0.20
M	Ti	0.56	Sputtered TFE	0.04
N	Ti	0.56	Sputtered TFE	0.08
O	Ti	0.56	Sputtered TFE	0.20

* Discontinuous

Table III. Summary of Coatings

Tube	Material	OD mm	ID mm	Wall Thickness mm	Type of Coating	Coating Thickness, microns	Droptwise Performance	$\frac{H_o}{H_{o(2)}} (2\pi V/s)$	$\frac{DC}{DC_{UN}}$ (2πV/s)	H_o (W/m ² °C)	Standard Deviation of H_o (W/m ² °C)	Steady-State Coefficient
FULL LENGTH TUBES												
A	90/10 CuNi	15.90	13.39	1.24	NRL Fluoropoly	12.70	excellent*	0.82	0.86	7311	186	0.026±.002
C	90/10 CuNi	15.90	13.39	1.24	NRL Fluoropoly	1.27	poor	1.41	1.24	12624	1490	" "
F	90/10 CuNi	15.90	13.39	1.24	NRL Fluoropoly	0.02	poor	1.07	1.00	9578	590	" "
G	90/10 CuNi	15.90	13.39	1.24	NEOX	5.0	excellent	1.53	1.27	13679	1670	" "
H	Al	15.90		2.54	CANEDIZING	7.5	poor	1.31	1.17	11725	672	" "
I	Ti	16.00		0.56	TUFRAI	10.0	poor	0.84	0.86	7554	492	" "
X	90/10 CuNi	15.90	13.39	1.24	UNKNOWNED	-	-	1.00	1.00	8943	1201	" "
SHORT TUBES												
J	90/10 CuNi	15.90		1.24	Sputtered TFE	0.20	excellent	1.04	0.93	10364	489	0.029±.003
K	90/10 CuNi	15.90		1.24	Sputtered TFE	0.08	excellent	1.45	1.21	14182	2223	" "
L	90/10 CuNi	15.90		1.24	Sputtered TFE	0.04	excellent	1.35	1.08	13435	1580	" "
M	Ti	15.90		0.56	Sputtered TFE	0.20	excellent	0.64	0.74	6390	864	" "
O	Ti	15.90		0.56	Sputtered TFE	0.04	excellent	1.00	0.96	9942	1409	" "
Z	90/10 CuNi	15.90		1.24	UNKNOWNED	-	-	1.00	1.00	9929	771	" "

TABLE IV. Summary of Coated Tube Characteristics and Performance

$\%$ Flow	T_v ($^{\circ}\text{C}$)	T_w ($^{\circ}\text{K}$)	T_{c_i} ($^{\circ}\text{C}$)	T_{c_o} ($^{\circ}\text{C}$)	ΔP (kPa)
10	65.89	316.78	10.64	21.47	1.0500
15	65.46	312.00	8.80	18.21	2.0394
15	67.47	312.01	9.86	19.17	2.1966
20	66.03	309.30	9.60	18.51	3.7650
30	67.43	304.98	9.38	15.86	7.8444
30	65.43	304.52	8.88	15.24	7.8444
40	66.38	302.44	9.20	14.53	13.0097
50	66.57	301.08	9.44	13.86	19.9241
50	65.44	300.52	8.90	13.39	19.4532
60	66.31	300.14	9.44	13.23	27.2976
70	65.84	299.62	9.30	12.71	35.6123
80	65.62	298.64	9.16	12.26	45.1817

TABLE V. Raw Data for Uncoated (Long) CuNi
Tube. 3 Feb 79.

$\frac{g}{\text{Flow}}$	$T_v (^{\circ}\text{C})$	$T_w (^{\circ}\text{K})$	$Tc_i (^{\circ}\text{C})$	$Tc_o (^{\circ}\text{C})$	$\Delta P (\text{kPa})$
10	65.96	325.48	12.02	21.59	1.2548
10	65.41	324.82	11.28	20.77	1.0355
15	65.96	322.84	11.80	19.77	2.5730
15	65.38	321.37	11.44	19.25	2.3537
20	66.15	321.09	11.60	18.53	4.2359
20	65.46	320.98	11.74	18.41	4.1415
25	65.82	320.50	11.60	17.59	5.9616
25	65.58	319.90	11.80	17.73	6.1181
30	65.81	319.67	11.60	16.94	8.3146
40	65.90	318.27	11.60	16.06	13.6488
50	65.97	317.95	11.66	14.45	20.7087
50	65.67	317.36	11.66	15.35	20.5515
60	65.78	316.96	11.70	14.97	28.8661
70	65.77	316.37	11.68	14.59	37.6516
80	65.97	315.57	11.70	14.33	47.8491

TABLE VI. Raw Data for 12.7 μm NRL Fluoroepoxy
Coated CuNi Tube. 5 Feb 79.

³ Flow	T _V (°C)	T _w (°K)	Tc _i (°C)	Tc _o (°C)	ΔP (kPa)
10	67.87	318.90	13.30	23.82	1.0748
10	66.91	319.73	14.40	24.50	1.0748
15	67.15	314.38	13.20	22.18	2.1966
15	66.95	316.01	14.28	22.84	2.2903
20	67.54	310.96	13.20	20.93	3.9222
20	67.01	312.39	14.10	21.73	3.7967
30	67.31	307.26	13.10	19.17	8.0009
40	67.12	303.76	13.20	18.16	13.7116
40	66.93	304.17	13.88	18.79	13.7116
50	67.20	302.56	13.26	17.59	20.1123
60	67.11	301.48	13.40	17.17	28.2070
60	67.12	301.29	13.68	17.41	27.6424
70	67.17	300.29	13.48	16.78	37.4945
80	67.22	299.23	13.52	16.51	50.6731

TABLE VII. Raw Data for 0.02 μm NRL Fluorocopoly
Coated CuNi Tube. 8 Feb 79.

³ Flow	T _v (°C)	T _w (°K)	Tc _i (°C)	Tc _o (°C)	ΔP (kPa)
10	62.83	322.36	13.16	24.59	1.1610
10	66.39	322.30	13.84	25.18	1.3175
15	62.94	318.73	12.84	22.68	2.4158
15	66.37	318.69	14.00	23.71	2.3531
20	63.46	316.10	12.62	21.36	4.0787
20	66.33	316.29	14.06	22.63	4.0787
30	64.64	313.16	12.72	19.79	8.3146
40	65.08	310.62	13.12	18.98	13.7116
40	65.67	310.36	14.06	19.75	14.0563
50	65.67	309.75	13.34	18.32	20.0806
60	65.83	308.48	13.52	17.78	28.2387
70	65.82	306.77	13.82	17.63	37.9653
80	65.99	307.41	14.04	17.44	48.4765

TABLE VIII. Raw Data for 1.27 μm NRL Fluoroepoxy Coated CuNi Tube. 9 Feb 79.

$\frac{3}{\text{Flow}}$	T_V ($^{\circ}\text{C}$)	T_W ($^{\circ}\text{K}$)	T_{C_i} ($^{\circ}\text{C}$)	T_{C_o} ($^{\circ}\text{C}$)	ΔP (kPa)
10	63.79	326.28	13.60	25.01	0.9411
10	66.26	327.34	17.50	28.30	1.0038
15	63.88	323.56	13.58	23.52	2.3531
15	66.34	325.44	17.48	26.79	2.1966
20	63.46	321.46	13.80	22.56	3.9222
20	66.31	323.23	17.32	25.59	3.6713
30	64.88	317.78	14.18	21.29	8.0009
40	65.83	315.49	14.62	20.54	13.4916
40	66.33	316.85	17.00	22.60	13.0214
50	66.01	311.66	14.98	20.00	20.4577
60	66.00	311.59	15.60	19.86	30.6207
60	66.36	312.09	16.70	20.94	30.6207
70	66.22	309.28	15.96	19.77	38.2790
80	66.33	307.08	16.30	19.67	48.3821

TABLE IX. Raw Data for "Nedox" Coated CuNi Tube.
10 Feb 79.

$\frac{3}{8}$ Flow	T _V (°C)	T _W (°K)	Tc _i (°C)	Tc _O (°C)	ΔP (kPa)
10	64.20	319.51	14.68	24.61	0.9101
10	66.42	319.61	17.62	27.13	1.0479
15	66.55	316.50	14.50	23.22	1.5692
15	66.32	316.07	16.93	25.11	1.8829
20	66.07	316.30	14.56	22.13	2.6668
30	66.59	313.65	14.94	21.11	5.4280
30	66.46	312.72	16.54	22.41	4.2359
40	66.14	311.10	15.20	20.22	9.0675
50	66.33	309.42	15.60	19.95	13.4909
50	66.53	310.35	16.12	20.46	13.4909
60	66.46	309.03	15.76	19.57	18.9830
70	66.53	308.06	15.80	19.24	24.9439

TABLE X. Raw Data for "Canadizing" Coated Ti Tube.
12 Feb 79.

^g Flow	T _v (°C)	T _w (°K)	Tc _i (°C)	Tc _o (°C)	ΔP (kPa)
10	62.95	316.74	13.58	23.85	1.0983
10	66.69	316.67	14.50	24.59	1.1610
15	63.87	311.79	13.60	22.23	2.1966
15	66.53	312.15	14.50	23.03	2.3220
20	65.07	308.47	13.64	21.20	3.8595
20	66.65	308.97	14.50	21.90	3.8278
30	65.32	304.37	13.86	19.83	7.3736
40	65.92	301.53	14.00	18.96	13.1152
40	66.78	301.99	14.80	19.65	13.5544
50	66.03	299.81	14.16	18.39	19.8296
60	66.17	298.35	14.30	18.00	28.4897
60	66.34	298.75	14.60	18.33	28.3959
70	66.25	297.55	14.38	17.65	37.4945
80	66.34	296.73	14.42	17.37	48.3193

TABLE XI. Raw Data for "Tufam" Coated Al Tube.
18 Feb 79.

³ Flow	T _v (°C)	T _w (°K)	Tc _i (°C)	Tc _o (°C)	ΔP (kPa)
10	67.91	320.30	15.38	18.25	1.2548
15	67.77	316.86	14.92	17.26	2.6668
20	67.90	314.11	14.56	16.58	4.2359
25	68.03	312.15	14.30	16.05	6.4008
30	68.76	309.77	13.88	15.45	8.6600
30	68.40	309.98	13.23	14.84	8.7228
35	68.55	308.25	13.74	15.14	11.5467
35	68.36	308.98	13.32	14.77	11.2013
40	68.63	307.16	13.60	14.93	14.5589
50	68.62	305.39	13.53	14.64	21.3361
60	68.64	304.02	13.68	14.63	29.0861
70	68.62	302.61	13.42	14.31	38.4990

TABLE XII. Raw Data for 0.20 μm Sputtered TFE
Coated CuNi Tube. 19 Feb 79.

$\frac{3}{4}$ Flow	T_V ($^{\circ}\text{C}$)	T_W ($^{\circ}\text{K}$)	T_{C_i} ($^{\circ}\text{C}$)	T_{C_o} ($^{\circ}\text{C}$)	ΔP (kPa)
10	65.07	318.64	13.32	16.38	1.0983
10	67.22	321.54	12.20	15.32	0.9728
15	65.61	316.02	13.04	15.61	2.3531
15	67.13	317.70	12.16	14.71	2.4158
20	66.18	314.03	12.92	15.07	3.9850
20	67.28	314.55	12.20	14.32	4.0477
25	66.43	312.12	12.82	14.75	5.9616
25	66.92	313.10	12.26	14.14	6.0243
30	66.51	310.54	12.80	14.52	8.3774
30	66.97	310.51	12.30	14.01	8.2209
35	66.65	310.00	12.78	14.30	11.1386
35	67.08	310.49	12.36	13.91	11.0758
40	66.51	307.97	12.74	14.18	13.8370
40	67.19	308.54	12.46	13.85	13.9625
50	66.68	305.67	12.70	13.97	20.8024
60	67.22	303.71	12.70	13.76	28.6779
70	67.22	302.98	12.68	13.61	37.5572
80	67.30	301.83	12.52	13.39	48.1311

TABLE XIII. Raw Data for 0.04 μm Sputtered TFE
Coated CuNi Tube. 22 Feb 79.

$\frac{g}{\text{Flow}}$	$T_V (^{\circ}\text{C})$	$T_W (^{\circ}\text{K})$	$T_{C_i} (^{\circ}\text{C})$	$T_{C_o} (^{\circ}\text{C})$	$\Delta P (\text{kPa})$
10	62.91	325.38	13.60	16.58	0.7218
15	63.64	324.44	13.10	15.49	1.5692
15	65.71	325.04	11.50	13.95	1.6319
20	64.08	323.39	12.68	14.71	2.9804
20	65.80	324.36	11.50	13.56	2.9177
25	65.63	323.03	11.44	13.25	4.2987
30	64.69	323.10	12.32	14.13	6.2436
30	65.67	321.00	11.40	13.08	6.2436
35	65.21	320.52	12.08	13.50	8.0637
35	65.58	320.02	11.42	12.87	8.0637
40	65.36	319.91	11.82	13.17	10.4484
40	65.63	319.59	11.54	12.88	10.4484
50	65.42	319.56	11.70	12.83	15.4055
60	66.16	319.04	11.54	12.55	21.0224
70	65.86	317.70	11.44	12.31	27.8933
80	65.80	316.63	11.40	12.15	35.5495

TABLE XIV. Raw Data for 0.20 μm Sputtered TFE Coated Ti Tube. 24 Feb 79.

$\frac{8}{\text{Flow}}$	T_v ($^{\circ}\text{C}$)	T_w ($^{\circ}\text{K}$)	T_{c_i} ($^{\circ}\text{C}$)	T_{c_o} ($^{\circ}\text{C}$)	ΔP (kPa)
10	64.53	322.36	13.84	17.21	1.0666
10	68.42	323.26	13.64	16.97	1.0666
15	65.49	320.06	13.56	16.25	2.3848
15	68.34	317.06	13.60	16.28	2.6350
20	66.94	317.06	13.30	15.68	3.8905
20	68.37	317.91	13.58	15.89	3.3259
25	66.87	314.87	13.24	15.28	6.2436
25	67.87	315.72	13.60	15.64	6.3380
30	66.82	314.08	13.26	15.02	8.5346
30	67.55	314.43	13.52	15.35	8.5346
35	67.72	312.49	13.22	14.85	11.2958
35	67.56	313.38	13.50	15.13	11.1703
40	67.65	312.26	13.20	14.75	14.3431
40	67.55	312.51	13.44	14.95	14.1190
50	67.78	310.38	13.24	14.57	21.1479
60	67.89	309.39	13.30	14.47	28.9916
70	67.76	308.69	13.36	14.37	38.2480
80	67.78	307.37	13.40	14.32	48.9474

TABLE XV. Raw Data for 0.08 μm Sputtered TFE Coated CuNi Tube. 26 Feb 79.

$\frac{3}{8}$ Flow	T _V (°C)	T _W (°K)	Tc _i (°C)	Tc _O (°C)	ΔP (kPa)
10	63.89	325.06	14.58	17.88	0.7218
10	67.56	323.14	12.96	16.25	0.7218
15	65.03	321.28	14.30	16.95	1.5692
15	67.52	320.00	12.96	15.65	1.6319
20	65.43	318.37	14.04	16.28	2.9804
20	67.44	317.20	13.02	15.28	2.9177
25	66.08	315.39	13.82	15.84	4.2987
25	67.44	315.28	13.10	15.06	4.4869
30	66.60	314.50	13.70	15.47	6.2436
30	67.52	313.46	13.12	14.92	6.2436
35	66.80	312.68	13.60	15.24	8.0637
35	67.57	312.64	13.18	14.83	8.0637
40	66.92	311.90	13.52	15.03	10.4484
40	67.66	312.02	13.26	14.78	10.4484
50	67.03	310.20	13.52	14.83	15.4055
60	67.69	309.48	13.48	14.63	21.0224
70	67.56	308.29	13.50	14.51	27.8933
80	67.61	307.58	13.42	14.35	35.5495

TABLE XVI. Raw Data for 0.04 μm Sputtered TFE Coated Ti Tube. 27 Feb 79.

$\frac{8}{\text{Flow}}$	T_v ($^{\circ}\text{C}$)	T_w ($^{\circ}\text{K}$)	Tc_i ($^{\circ}\text{C}$)	Tc_o ($^{\circ}\text{C}$)	ΔP (kPa)
10	65.66	330.20	14.32	17.39	1.0983
10	67.27	319.87	13.30	16.45	1.2238
15	66.10	328.08	14.14	16.65	2.4475
15	67.34	316.96	13.30	15.84	2.5730
20	66.23	327.96	14.02	16.14	4.2987
20	67.26	315.12	13.30	15.45	4.2987
25	66.40	326.59	13.90	15.81	6.2753
25	67.22	314.03	13.35	15.23	6.6834
30	66.68	326.41	13.90	15.54	8.8165
30	66.81	312.84	13.44	15.12	8.9420
35	66.69	324.57	13.88	15.35	11.7660
35	66.25	312.06	13.48	14.99	12.0797
40	66.82	325.37	13.90	15.22	15.2173
40	65.94	313.29	13.72	15.07	15.2800
50	66.97	323.61	13.92	15.06	23.0617
60	66.96	323.49	13.92	14.93	31.4708
70	67.16	322.73	14.08	14.93	41.5111
80	67.08	320.36	13.94	14.73	54.3754

TABLE XVII. Raw Data for Uncoated (short) CuNi Tube. 28 Feb 79.

Velocity	Reynolds Number	UN	UC	Sieder Tate Constant	H _i	H _O
0.86	10664.86	2372.761	2570.039	0.02802090	4593.425	7816.183
1.29	15073.69	2964.257	3278.668	0.02821952	6172.447	9037.365
1.29	15434.07	2875.430	3170.342	0.02814037	6213.506	8172.777
1.72	20360.25	3741.460	4256.685	0.02817609	7741.685	12504.824
2.59	29518.59	3865.838	4418.417	0.02829040	10481.327	8938.734
2.59	29129.56	3899.939	4463.020	0.02833515	10429.117	9171.128
3.45	38658.83	4267.667	4951.247	0.02835089	13033.130	9097.053
4.31	48072.75	4389.951	5116.601	0.02836848	15496.652	8472.356
4.31	47490.60	4508.043	5277.741	0.02840972	15418.829	8954.717
5.17	57256.81	4515.841	5288.432	0.02839482	17843.230	8206.065
6.04	66263.98	4739.992	5598.474	0.02842110	20109.197	8405.833
6.90	75181.84	4916.762	5846.751	0.02833576	22265.821	8535.472

TABLE VXIII. Results of Uncoated (long) CuNi Tube. 3 Feb 79.

Velocity	Reynolds Number	UN	UC	Sieder Tate Constant	H _i	H _o
0.86	10850.01	2123.340	2279.954	0.02376128	4002.962	7198.223
0.86	10658.03	2096.792	2249.373	0.02381161	3976.915	6996.759
1.29	15897.16	2593.481	2831.006	0.02382754	5466.354	7475.136
1.29	15736.50	2550.309	2779.642	0.02385627	5431.673	7199.277
1.72	20844.39	2955.263	3267.668	0.02387491	6820.096	7684.370
1.72	20852.47	2883.331	3179.950	0.02387382	6818.984	7217.751
2.16	25773.60	3183.758	3549.328	0.02390578	8116.707	7465.606
2.16	25874.07	3176.653	3540.500	0.02389473	8113.527	7429.854
2.59	30696.01	3384.836	3801.060	0.02392720	9352.425	7417.484
3.45	40503.01	3727.818	4239.035	0.02395691	11697.788	7498.946
4.31	50304.98	2942.355	4516.655	0.02397520	13947.819	7391.129
4.81	50245.65	3844.860	4391.035	0.02397857	13922.802	7063.405
5.17	60057.78	4077.564	4697.179	0.02398981	16074.999	7232.355
6.04	69727.29	4216.913	4883.061	0.02400370	18133.332	7212.223
6.90	79457.74	4323.630	5026.732	0.02401198	20119.980	7178.067

TABLE XIX. Results of 12.7 μ m NRL Fluoroepoxy Coated
CuNi Tube. 5 Feb 79.

Velocity	Reynolds Number	UN	UC	Sieder Tate Constant	H _i	H _O
0.86	11290.59	2326.008	2515.278	0.02495515	4203.642	8913.055
0.86	11443.89	2318.619	2506.639	0.02489658	4229.834	8670.603
1.29	16605.66	2990.351	3310.620	0.02501332	5716.659	10844.509
1.29	16826.77	2889.548	3187.514	0.02495515	5764.223	9468.800
1.72	21827.04	3333.737	3736.740	0.02505563	7103.240	10128.639
1.72	22108.35	3382.061	3797.559	0.02499844	7158.958	10442.941
2.59	32056.01	3875.180	4430.624	0.02511844	9669.539	9838.602
3.45	42009.28	4198.871	4858.886	0.02515015	12001.054	9447.397
3.45	42655.92	4228.880	4899.115	0.02510475	12066.077	9551.287
4.31	52201.06	4548.299	5333.001	0.02516780	14261.573	9671.515
5.17	62447.36	4752.384	5615.770	0.02517704	16435.308	9516.579
5.17	62819.33	4725.298	5577.988	0.02515935	16467.291	9396.050
6.04	72582.44	4829.801	5724.192	0.02518823	18524.048	9096.102
6.90	82736.73	4984.465	5942.738	0.02519595	20533.018	9103.418

TABLE XX. Results of 0.02 μ m NRL Fluoroepoxy Coated CuNi Tube. 8 Feb 79.

Velocity	Reynolds Number	UN	UC	Sieder Tate Constant	H _i	H _O
0.86	11371.12	2838.988	3126.099	0.02863815	4882.234	13481.269
0.86	11533.17	2638.116	2884.275	0.02859034	4900.752	9811.081
1.29	16632.86	3562.691	4026.803	0.02872346	6646.616	14738.240
1.29	17048.19	3340.111	3744.751	0.02863983	6691.692	11393.286
1.72	21791.10	4099.586	4726.426	0.02878323	8271.094	15028.747
1.72	22471.34	3915.832	4483.846	0.02867873	8246.079	12612.134
3.59	32142.15	4772.121	5643.350	0.02884058	11300.981	14074.952
3.45	42653.97	5200.507	6252.414	0.02885675	14111.714	13345.847
3.45	43499.35	5077.060	6074.831	0.02878971	14179.004	12498.667
4.31	53044.94	5440.656	6602.811	0.02887430	16806.267	12488.831
5.17	63393.01	5537.165	6745.494	0.02888837	19356.241	11591.323
6.04	74091.60	5785.290	7117.364	0.02888221	21805.087	11697.819
6.90	84697.86	5898.570	7274.326	0.02888133	24308.014	11348.273

TABLE XXI. Results of 1.27 μ m NRL Fluoroepoxy Coated
CuNi Tube. 9 Feb 79.

Velocity	Reynolds Number	UN	UC	Sieder Tate Constant	H _i	H _O
0.86	11480.44	2800.010	3078.904	0.02768710	4781.991	13526.374
0.86	12422.22	2712.917	2973.923	0.02743129	4899.874	10937.293
1.29	16931.65	3588.007	4059.174	0.02774250	6541.408	15881.222
12.9	18326.81	3437.534	3867.642	0.02748479	6716.564	12507.846
1.72	22387.06	4216.130	4882.011	0.02777001	8173.780	17220.690
1.72	24077.56	4008.131	4605.279	0.02753257	8376.291	13626.963
2.59	33244.79	4925.235	5858.736	0.02780304	11172.303	15795.007
3.45	44170.29	5336.018	6449.327	0.02781464	13968.547	14456.066
3.45	46430.09	5230.985	6296.521	0.02765115	14212.711	13438.439
4.31	55101.54	5627.821	6880.515	0.02782129	16523.672	13747.955
5.17	66481.21	5757.827	7075.844	0.02780345	19143.562	12712.668
5.17	68141.83	5812.358	7158.375	0.02772247	19300.814	12896.097
6.04	77805.77	5996.149	7439.203	0.02779311	21541.175	12701.067
6.90	89155.84	6064.282	7544.365	0.02778443	23843.304	12160.013

TABLE XXII. Results of "Nedox" Coated CuNi Tube. 10 Feb 79.

Velocity	Reynolds Number	UN	UC	Sieder Rate Constant	H _i	H _o
0.69	10372.88	3429.731	2649.106	0.02570484	3600.902	12698.982
0.69	11014.37	2348.108	2552.371	0.02552386	3662.345	10197.313
1.04	15289.52	2987.055	3325.623	0.02575798	4919.307	13192.122
1.04	16040.32	2946.723	3275.707	0.02561276	4979.865	11203.041
1.39	20150.72	3450.764	3910.701	0.02579334	6169.260	12294.222
2.08	20010.89	4147.094	4829.742	0.02581514	8458.339	12520.280
2.08	31003.39	4074.864	4732.057	0.02571610	8514.507	11766.976
2.77	39728.77	4510.547	5329.914	0.02583703	10554.921	11668.236
3.47	49756.04	4869.670	5838.720	0.02583241	12566.347	11673.206
3.47	50313.76	4887.887	5864.929	0.02579716	12638.303	11711.206
4.16	59533.14	5093.793	6163.897	0.02584011	14513.952	11348.421
4.85	69228.04	5338.805	6526.328	0.02585014	16260.714	11431.286

TABLE XXIII. Results of "Canadizing" Coated Ti Tube. 12 Feb 79.

Velocity	Reynolds Number	UN	UC	Sieder Tate Constant	H _i	H _O
0.83	11116.73	2512.745	2549.701	0.02680954	4349.715	8372.408
0.83	11324.38	2313.109	2344.390	0.02675102	4371.407	6445.754
1.25	16377.19	3043.540	3097.927	0.02686673	5910.099	8193.467
1.25	16691.74	2890.436	2939.446	0.02680638	5947.106	7107.251
1.66	21592.80	3427.851	3496.997	0.02690239	7305.306	8093.786
1.66	21976.47	3297.806	3361.756	0.02684640	7396.694	7295.960
2.49	31965.44	3986.273	4080.091	0.02694438	10014.966	7897.285
3.32	42264.24	4332.103	4443.132	0.02657120	12474.923	7694.650
3.32	42994.98	4223.809	4329.289	0.02691649	12551.317	7328.282
4.15	52588.25	4585.201	4709.770	0.02698588	14819.170	7560.671
4.98	62920.72	4789.038	4925.092	0.02699528	17057.858	7491.312
4.98	63380.21	4838.505	4977.425	0.02697201	17112.873	7600.125
5.81	73182.48	4920.032	5063.743	0.02700511	19233.826	7363.919
6.64	83401.76	5048.505	5199.935	0.02701414	21332.231	7315.673

TABLE XXIV. Results of "Tufram" Coated Al Tube. 18 Feb 79.

Velocity	Reynolds Number	UN	UC	Sieder Tate Constant	H _i	H _o
0.87	10915.62	2431.081	2638.600	0.02567430	4320.030	10030.724
1.31	16102.29	2996.879	3318.624	0.02572517	5896.980	10338.836
1.74	21215.18	3461.661	3898.211	0.02576158	7346.571	10835.058
2.18	26277.54	3732.724	4245.380	0.02578956	8715.278	10297.834
2.62	31159.95	3950.059	4528.780	0.02582604	9986.976	10000.369
2.62	30701.21	4064.534	4679.896	0.02587160	9951.524	10818.313
3.05	36160.26	4107.004	4736.289	0.02584238	11234.478	9639.716
3.05	35827.43	4293.221	4985.675	0.02587079	11227.876	10739.615
3.49	41159.63	4521.256	5295.860	0.02585477	12449.713	10880.001
4.36	51228.81	4711.350	5558.562	0.02586799	14791.898	10169.481
5.23	61578.86	4828.400	5722.224	0.02586277	17056.743	9613.627
6.11	71356.03	5373.786	6504.580	0.02586365	10181.349	11008.989

TABLE XXV. Results of 0.20 μ m Sputtered TFE Coated CuNi Tube.
19 Feb 79.

Velocity	Reynolds Number	UN	UC	Sieder Tate Constant	H _i	H _O
0.86	10371.10	2752.644	3021.729	0.02773582	4517.675	15291.009
0.86	10109.87	2596.589	2834.709	0.02782003	4517.751	11463.159
1.29	15367.99	3494.605	3940.038	0.02777605	6186.653	16694.282
1.29	15048.00	3237.713	3616.515	0.02784563	6176.676	12151.820
1.72	20331.04	3824.040	4363.900	0.02780188	7731.016	13516.523
1.72	19982.46	3580.461	4049.519	0.02785913	7704.318	10960.594
2.16	25287.91	4318.256	5019.469	0.02781830	9183.322	14578.456
2.16	24941.96	4046.917	4656.557	0.02786392	9171.733	11910.998
2.59	30258.23	4643.036	5463.717	0.02782783	10572.285	14376.579
2.59	29898.86	4493.658	5258.035	0.02796741	10536.424	13100.853
3.02	35198.64	4740.139	5598.679	0.02783738	11933.003	12806.674
3.02	34863.65	4758.515	5624.332	0.02786916	11916.843	12964.574
3.45	40154.35	5225.581	6289.127	0.02784346	13198.635	14681.018
3.45	39865.15	4856.313	5761.470	0.02786741	13192.554	12101.335
4.31	50041.58	5849.629	7214.993	0.02785346	15664.759	16123.908
5.17	59900.09	5706.760	6998.877	0.02786174	18011.897	13109.812
6.04	69745.65	5844.985	7207.929	0.02786829	20322.021	12546.148
6.90	79353.05	6251.676	7836.676	0.02788315	22510.091	13456.642

TABLE XXVI. Results of 0.04 μ m Sputtered TFE Coated CuNi Tube.
22 Feb 79.

Velocity	Reynolds Number	UN	UC	Sieder Tate Constant	H _i	H _O
0.69	9351.93	2300.792	2496.564	0.03098225	4224.629	6853.202
1.04	13770.18	2643.409	2905.144	0.03105057	5800.500	6298.733
1.04	13270.14	2484.699	2714.581	0.04118749	5749.226	5516.570
1.35	18103.19	2918.836	3241.281	0.03110266	7254.938	6240.473
1.35	17609.46	2750.117	3034.546	0.03140519	7215.944	5541.345
1.73	21915.76	3031.696	3381.050	0.04122145	8588.533	5864.620
2.08	26857.09	4001.340	4633.191	0.03114347	9997.151	9239.569
2.08	26232.67	3444.905	3903.179	0.03123083	9881.535	6786.932
2.43	31008.71	3375.255	3814.005	0.03118310	11206.589	6016.826
2.43	30535.74	3390.156	3833.043	0.03134934	11145.121	6080.873
2.77	35190.94	3692.763	4224.442	0.03120814	12427.104	6659.815
2.77	34953.68	3597.868	4100.713	0.03123330	12393.909	6366.795
3.47	43750.16	3775.389	4332.792	0.03122836	14820.643	6320.524
4.16	52221.83	4009.777	4644.507	0.03124814	17100.526	6561.604
4.85	60682.58	3993.077	4622.116	0.03126302	19255.079	6230.711
5.55	69185.28	3825.352	4398.862	0.03127197	21358.265	5650.820

TABLE XXVII. Results of 0.20 μ m Sputtered TFE Coated Ti Tube.
24 Feb 79.

Velocity	Reynolds Number	UN	UC	Sieder Tate Constant	H _i	H _O
0.86	10534.31	3252.981	3635.575	0.03177835	5255.882	21359.747
0.86	10480.18	2865.747	3158.575	0.03179729	5259.748	11297.058
1.29	15570.80	3769.813	4293.423	0.03183242	7179.748	15190.389
1.29	15588.89	3475.620	3915.922	0.03182948	7211.200	11234.296
1.72	20568.07	4345.620	5056.083	0.03186921	8972.112	15606.335
1.72	20685.85	4050.018	4660.662	0.03184760	9005.703	12291.734
3.16	25573.35	4647.015	5469.228	0.03188941	10650.333	14244.067
2.16	25790.33	4566.627	5358.216	0.03185741	10698.670	13433.518
2.59	30600.18	4760.981	5627.778	0.03190027	12287.710	12490.209
2.59	30812.03	4972.398	5925.593	0.03187413	12322.467	14004.125
3.02	35611.64	5101.542	6109.914	0.03190967	13833.349	12905.572
3.02	35849.32	5149.777	6179.231	0.03188448	13891.250	13249.465
3.45	40640.85	5653.250	6918.564	0.03191512	15277.544	15031.320
3.45	40853.45	5503.986	6696.318	0.03189533	15410.014	13988.115
4.31	50721.50	6106.574	7609.932	0.03193107	18283.149	15198.954
5.17	60833.99	6463.149	8171.763	0.03192305	21094.818	15266.058
6.04	70945.17	6479.885	8198.536	0.03192454	23815.537	13966.121
6.90	81069.59	6803.002	8722.715	0.03192504	26404.074	14448.737

TABLE XXVIII. Results of 0.08 μ m Sputtered TFE Coated CuNi Tube. 26 Feb 79.

Velocity	Reynolds Number	UN	UC	Sieder Tate Constant	H _i	H _O
0.69	9601.47	2674.488	2942.726	0.02883550	3970.254	14519.418
0.69	9247.18	2314.778	2513.040	0.02896445	3911.152	8137.862
1.04	14204.30	3080.697	3442.109	0.02888286	5421.301	10858.616
1.04	13773.76	2851.122	3157.993	0.02898862	5358.364	8628.177
1.39	18735.28	3399.000	3844.353	0.02891997	6755.320	9912.795
1.39	18298.16	3180.643	3567.358	0.02900118	6691.437	8364.204
1.73	23238.14	3794.926	4358.678	0.02894662	7997.687	10534.957
1.73	22833.96	3453.825	3914.633	0.02900703	7956.490	8316.008
2.08	27727.14	3905.604	4505.316	0.02896624	9217.810	9500.410
2.08	27365.02	3846.891	4427.368	0.02901153	9159.450	9223.148
2.43	32226.69	4228.108	4939.978	0.02897921	10367.396	10134.890
2.43	31913.36	4142.619	4823.674	0.02901288	10338.706	9684.582
2.77	36706.13	4425.196	5211.146	0.02899086	11501.768	10165.815
2.77	36486.70	4359.488	5120.265	0.02901153	11486.312	9837.767
3.47	45775.22	4814.134	5759.064	0.02899894	13678.597	10526.766
4.16	54772.91	5008.896	6040.017	0.02900883	15783.185	10266.344
4.85	63826.72	5134.700	6223.898	0.02901288	17791.239	9979.352
5.55	72735.52	5406.288	6627.456	0.02902279	19742.652	10373.467

TABLE XXIX. Results of 0.04 μ m Sputtered TFE Coated Ti Tube.
27 Feb 79.

Velocity	Reynolds Number	UN	UC	Sieder Tate Constant	H _i	H _O
0.86	10615.79	2745.185	3012.743	0.03173561	5361.379	9244.538
0.86	10379.19	2704.167	2963.411	0.03182162	5200.514	9365.372
1.29	15754.76	3360.315	3770.164	0.03177580	7358.375	9783.481
1.29	15456.13	3291.503	3683.759	0.03184808	7126.693	9696.064
1.72	20852.47	3747.796	4264.888	0.03180354	9241.223	9554.628
1.72	20514.73	3912.549	4479.541	0.03186628	8917.905	11271.488
2.16	25931.10	4279.847	4967.649	0.03182308	10998.761	10844.301
2.16	25590.00	4117.097	4749.717	0.03187318	10624.466	10242.948
2.59	31020.73	4306.228	5003.225	0.03183484	12707.373	9481.557
2.59	30700.00	4516.718	5289.634	0.03167417	12253.901	10970.648
3.02	36101.77	4522.700	5297.842	0.03184416	14303.822	9533.862
3.02	35779.38	4806.421	5691.381	0.03187812	13829.842	11240.460
3.45	41205.65	4590.209	5390.711	0.03184807	15940.556	9070.403
3.45	41045.34	4932.633	5869.207	0.03186382	15454.918	10780.460
4.31	51420.17	4974.926	5929.183	0.03185546	18968.212	9486.425
5.17	61616.06	5302.325	6400.173	0.03186087	21931.716	9847.559
6.04	72016.30	5124.063	6142.245	0.03185398	24777.724	8741.884
6.90	81973.30	5534.758	6741.922	0.03186924	27383.006	9567.833

TABLE XXX. Results of Uncoated (short) SuNi Tube. 28 Feb 79.

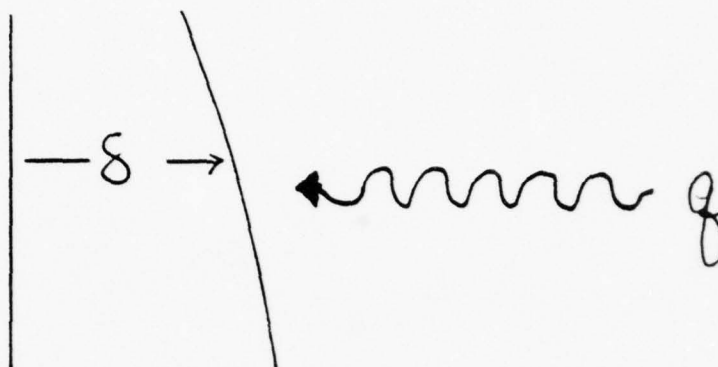


Figure 1a. Filmwise Mode

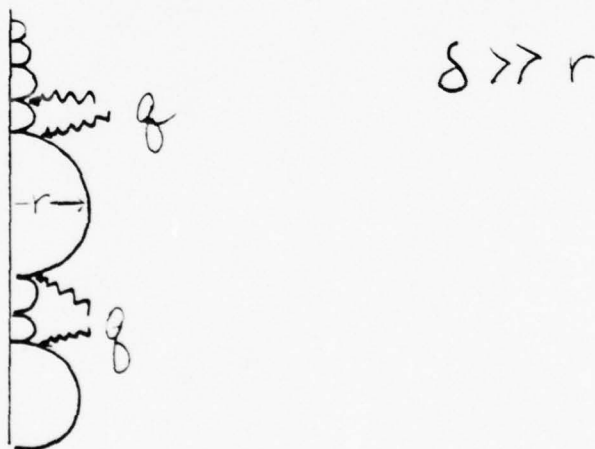


Figure 1b. Dropwise Mode

Figure 1. Comparison of Path of Heat Conduction of Dropwise versus Filmwise Condensation

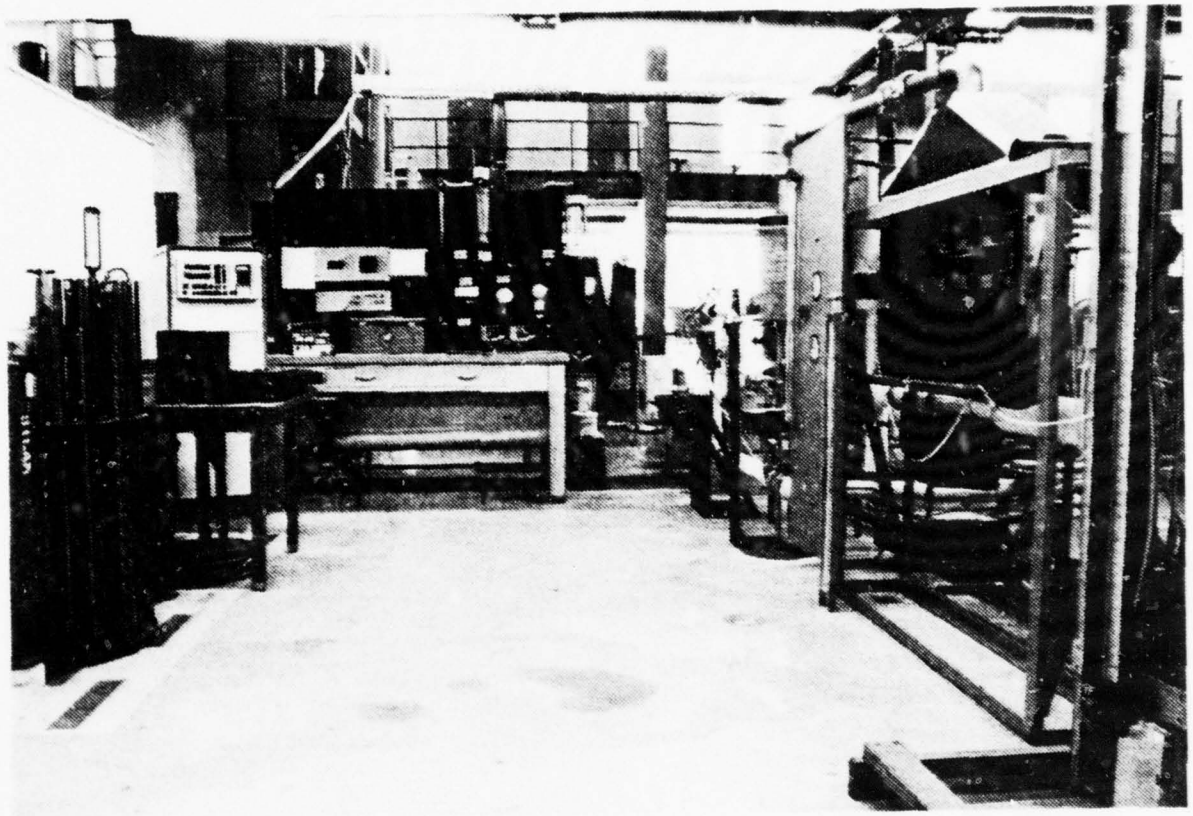
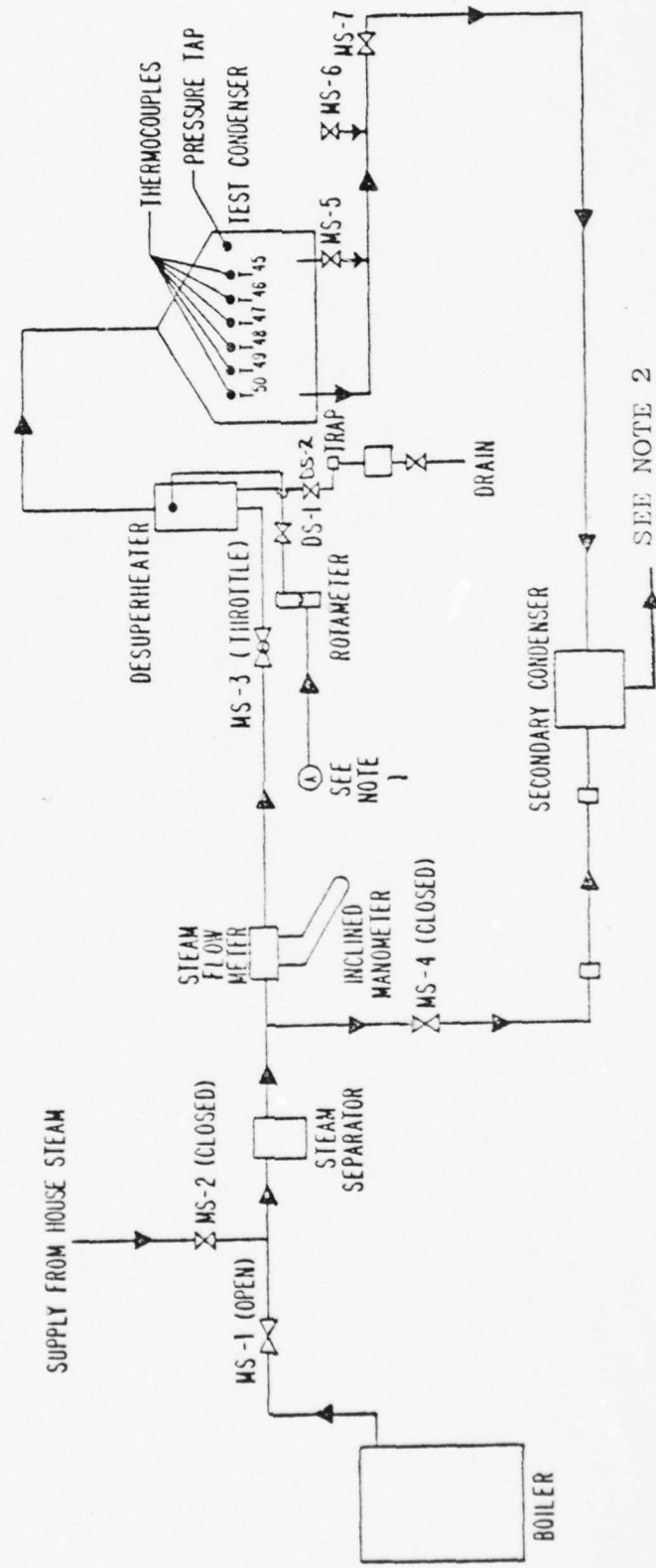


Figure 2. Photograph of Test Facility

STEAM SYSTEM



NOTE 1: From discharge of feed pump

NOTE 2: To air ejector via refrigerated cold trap and vacuum pump

Figure 3. Schematic Diagram of Steam System

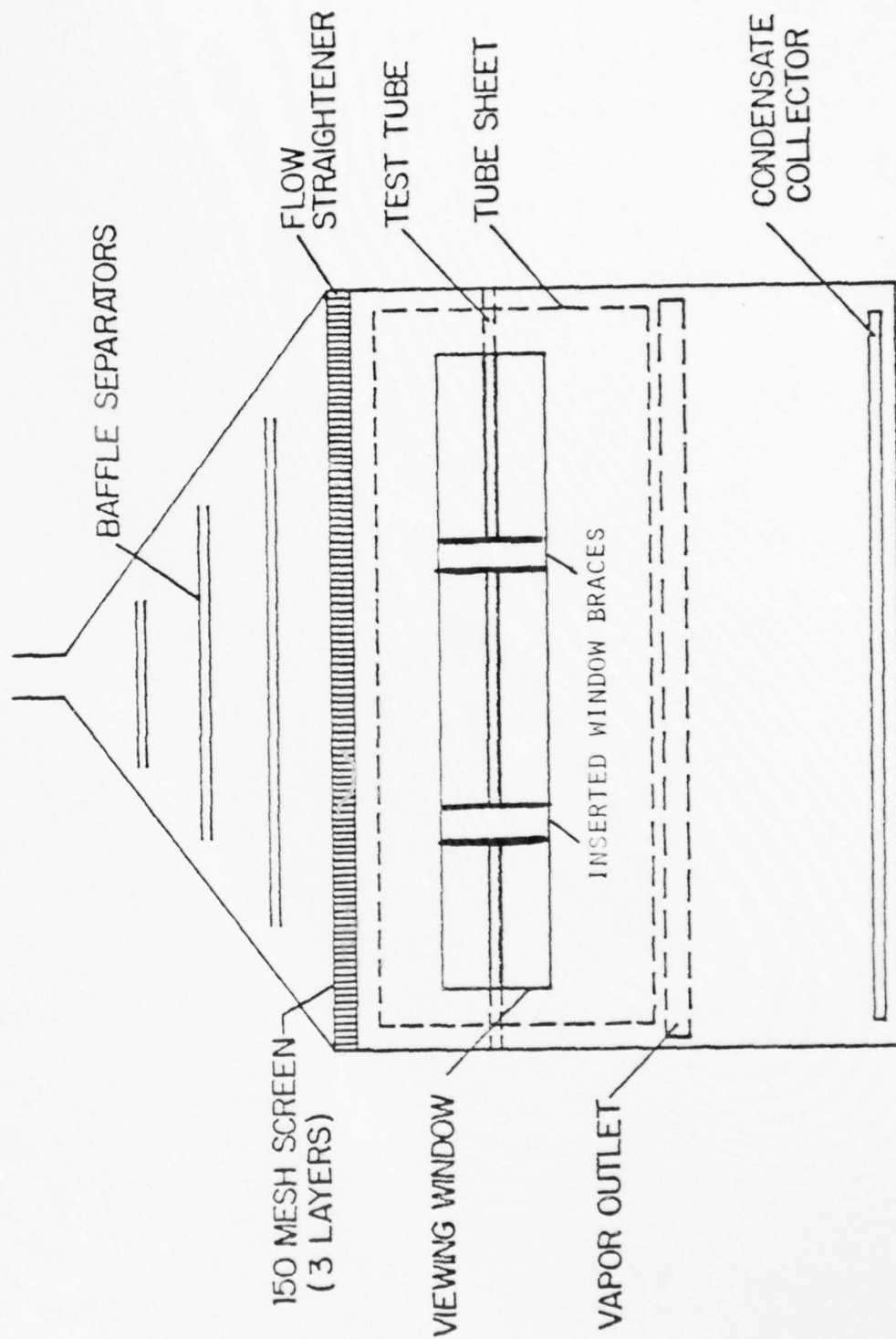


Figure 4. Test Condenser Schematic, Front View

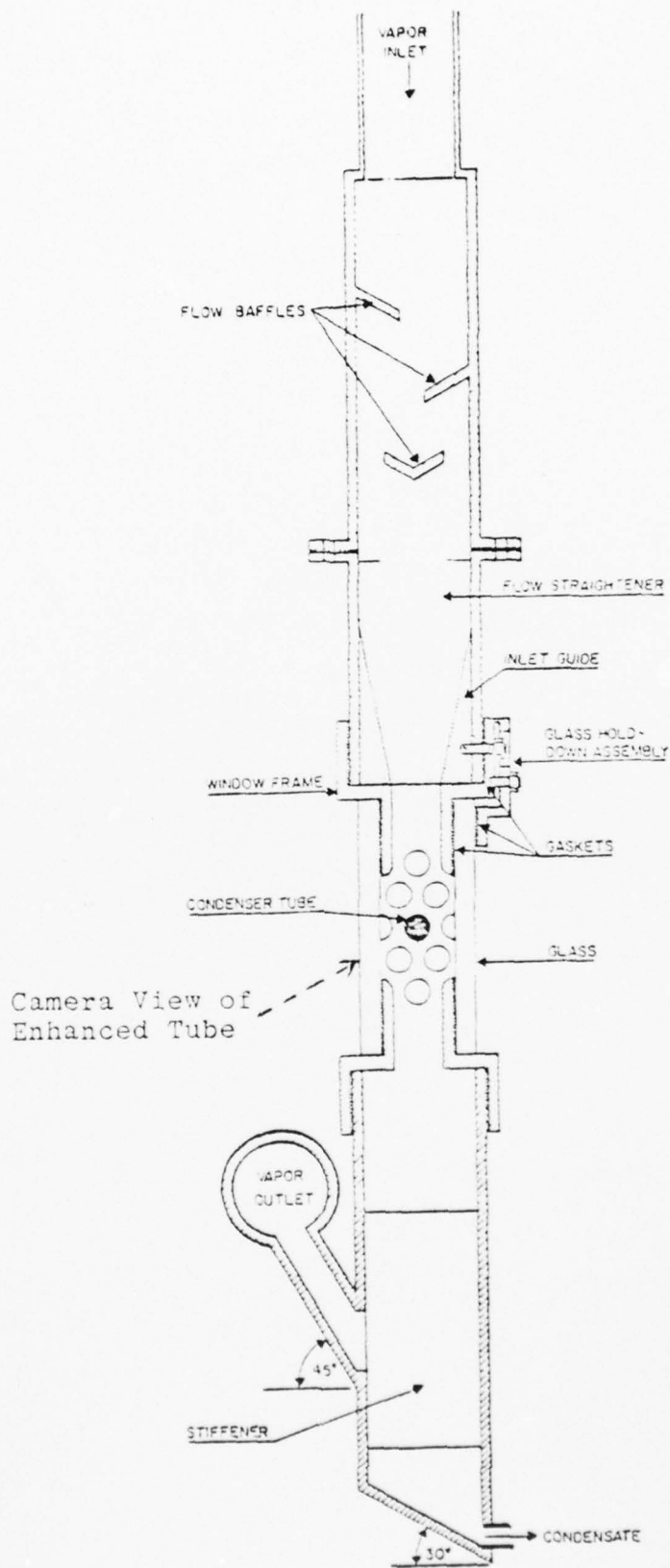


Figure 5. Test Condenser Schematic, Side View

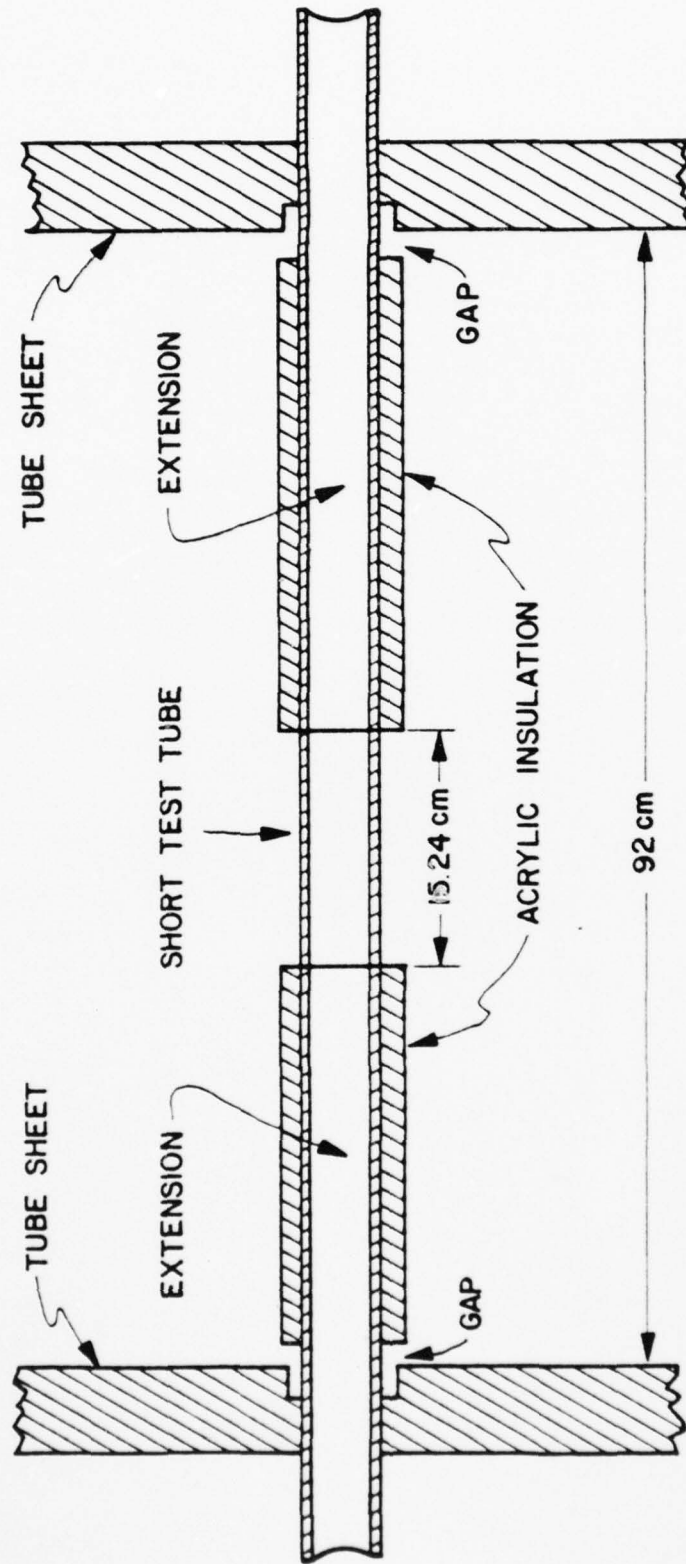


Figure 6. Diagram of short tube with insulated extensions inside test condenser without dummy tubes

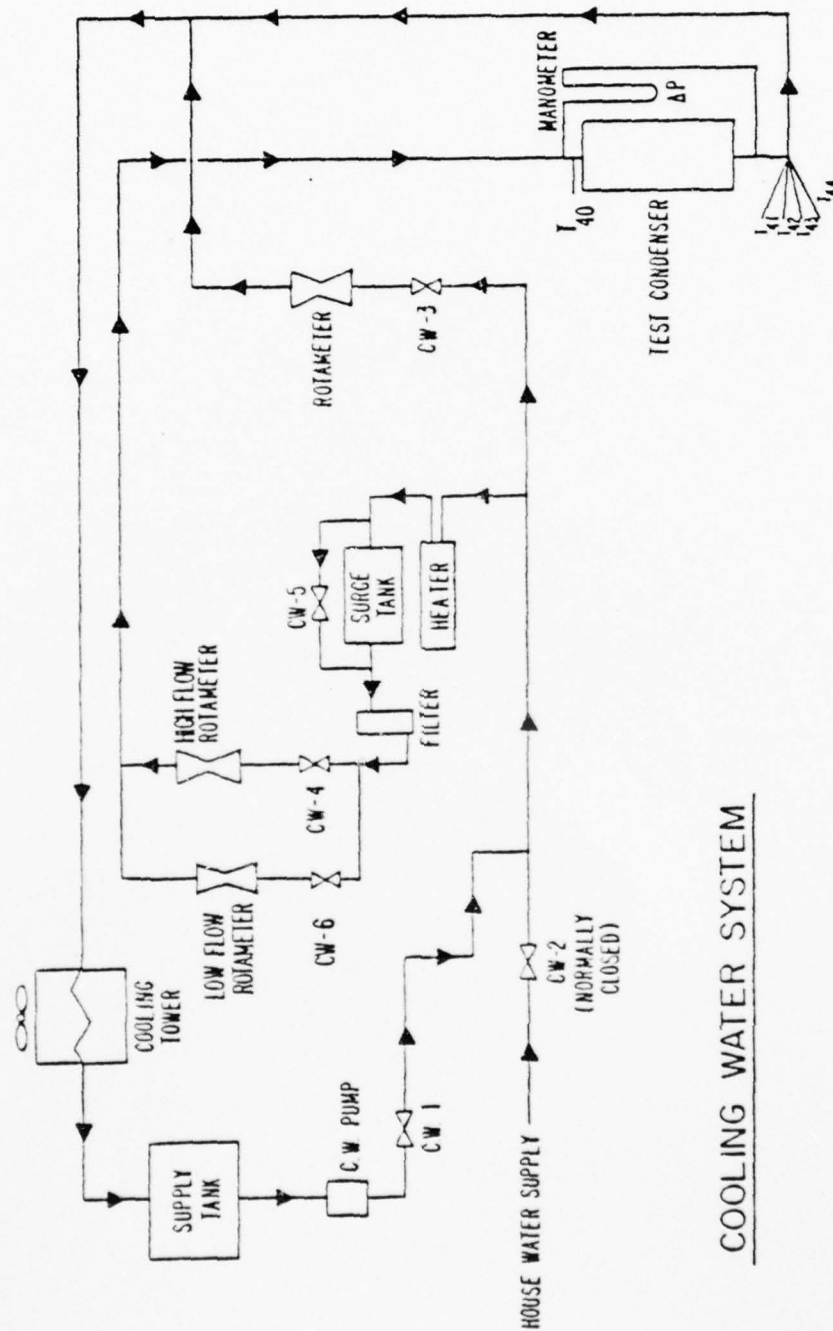


Figure 7. Schematic Diagram of Cooling Water System

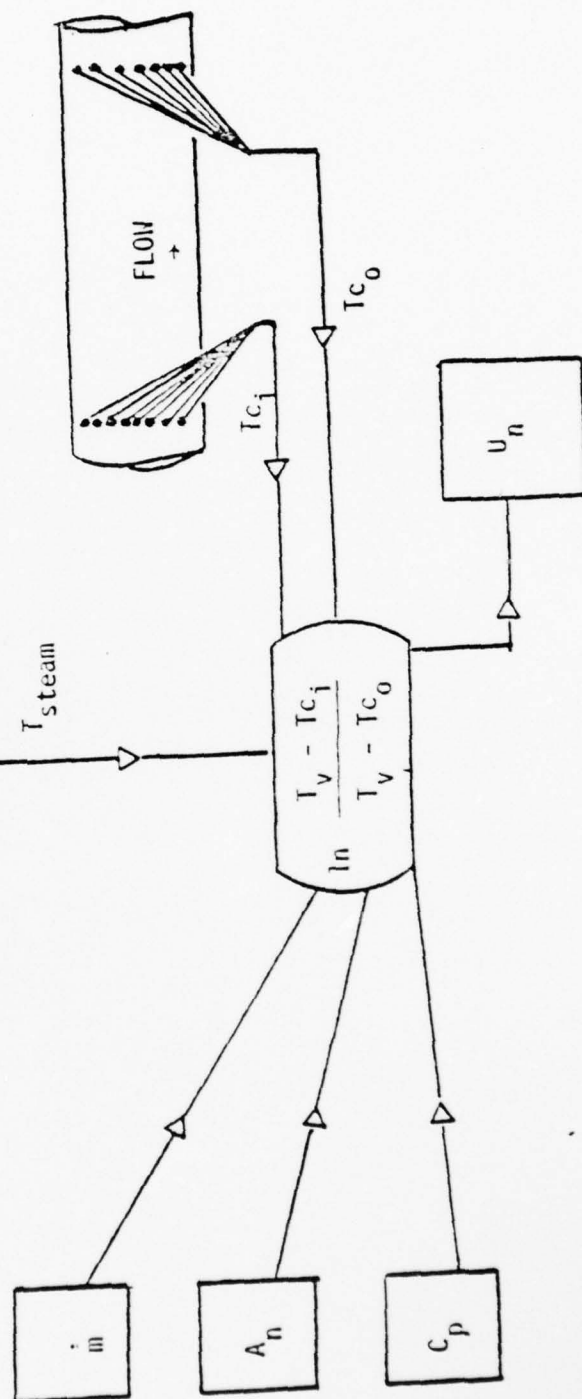


Figure 8. Schematic Representation of Procedure Used to Find U_n

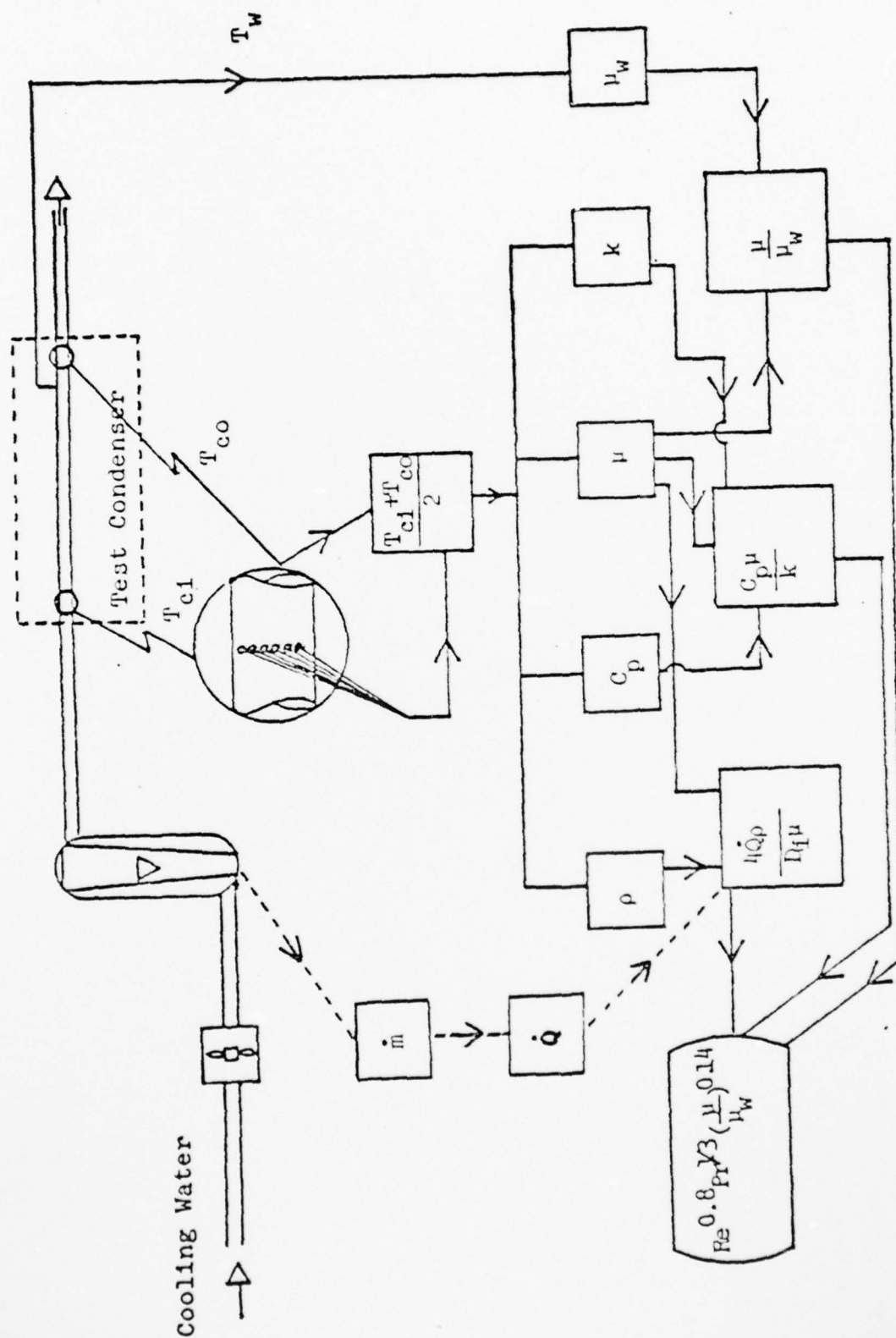


Figure 9. Schematic Representation of Procedure Used to Find Sieder-Tate Parameter

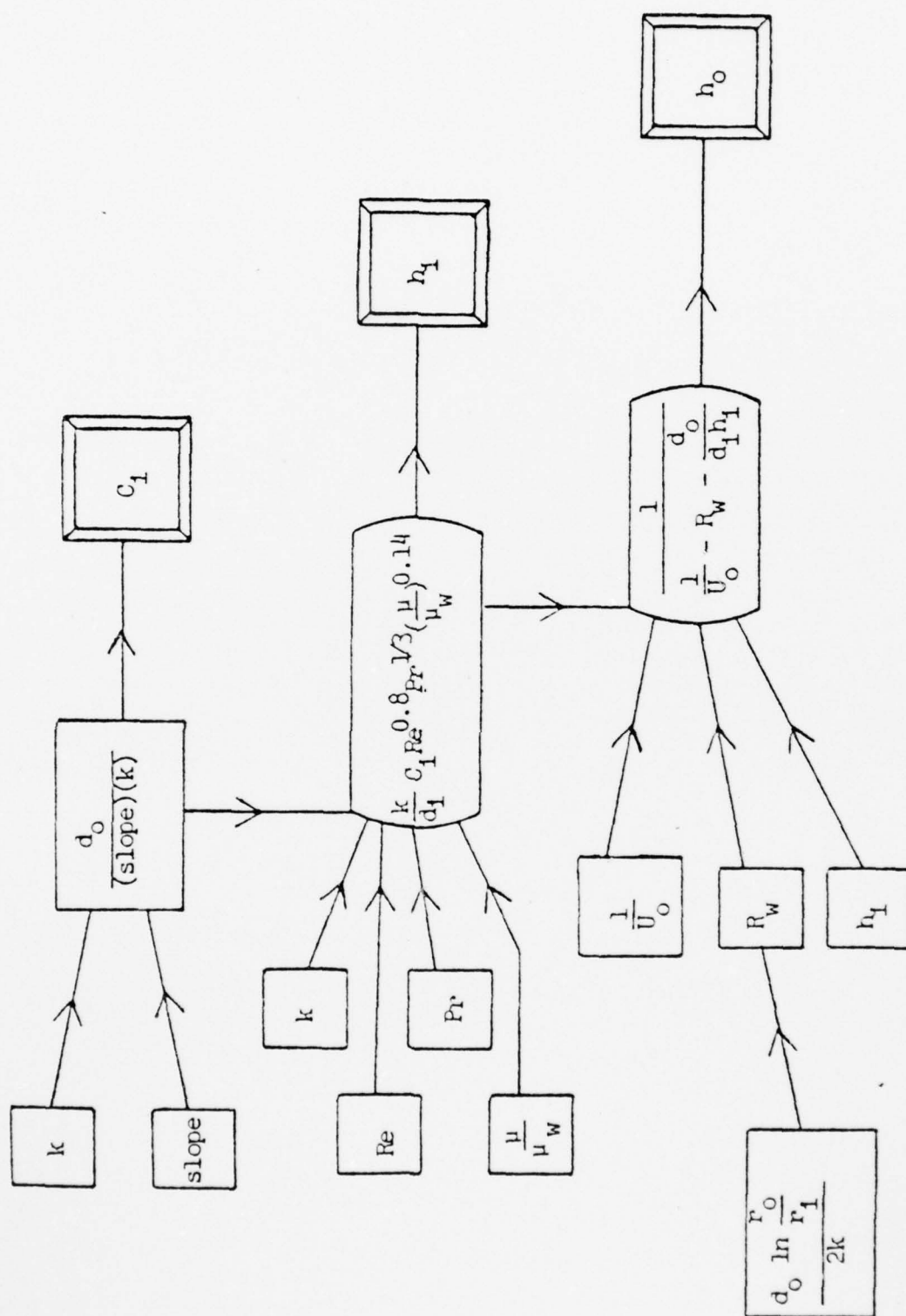


Figure 10. Schematic Representation of Procedure Used to Find Sieder-Tate Coefficient C_i , h_i and h_o

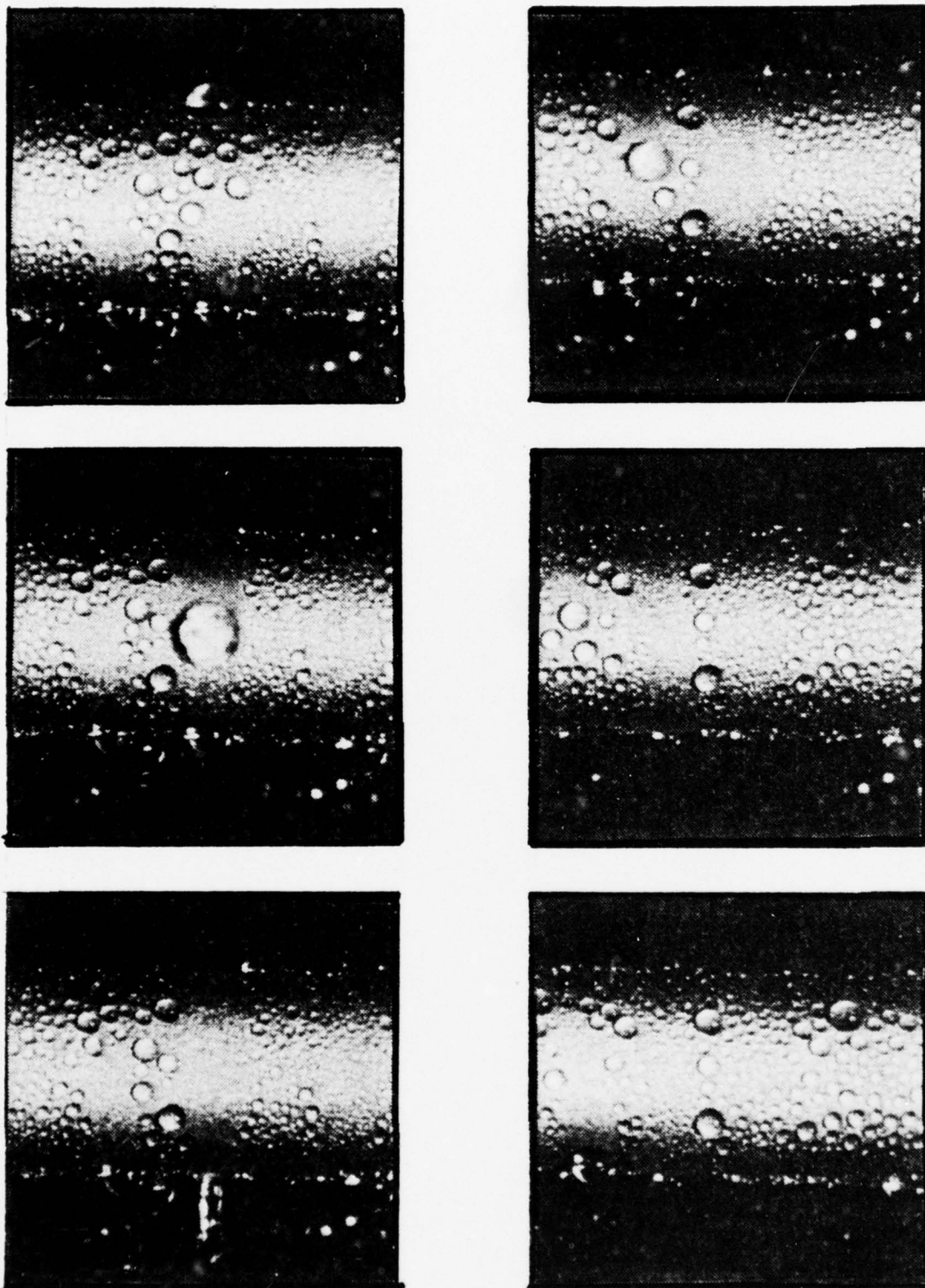


Figure 11. Film Sequence of Dropwise Condensation

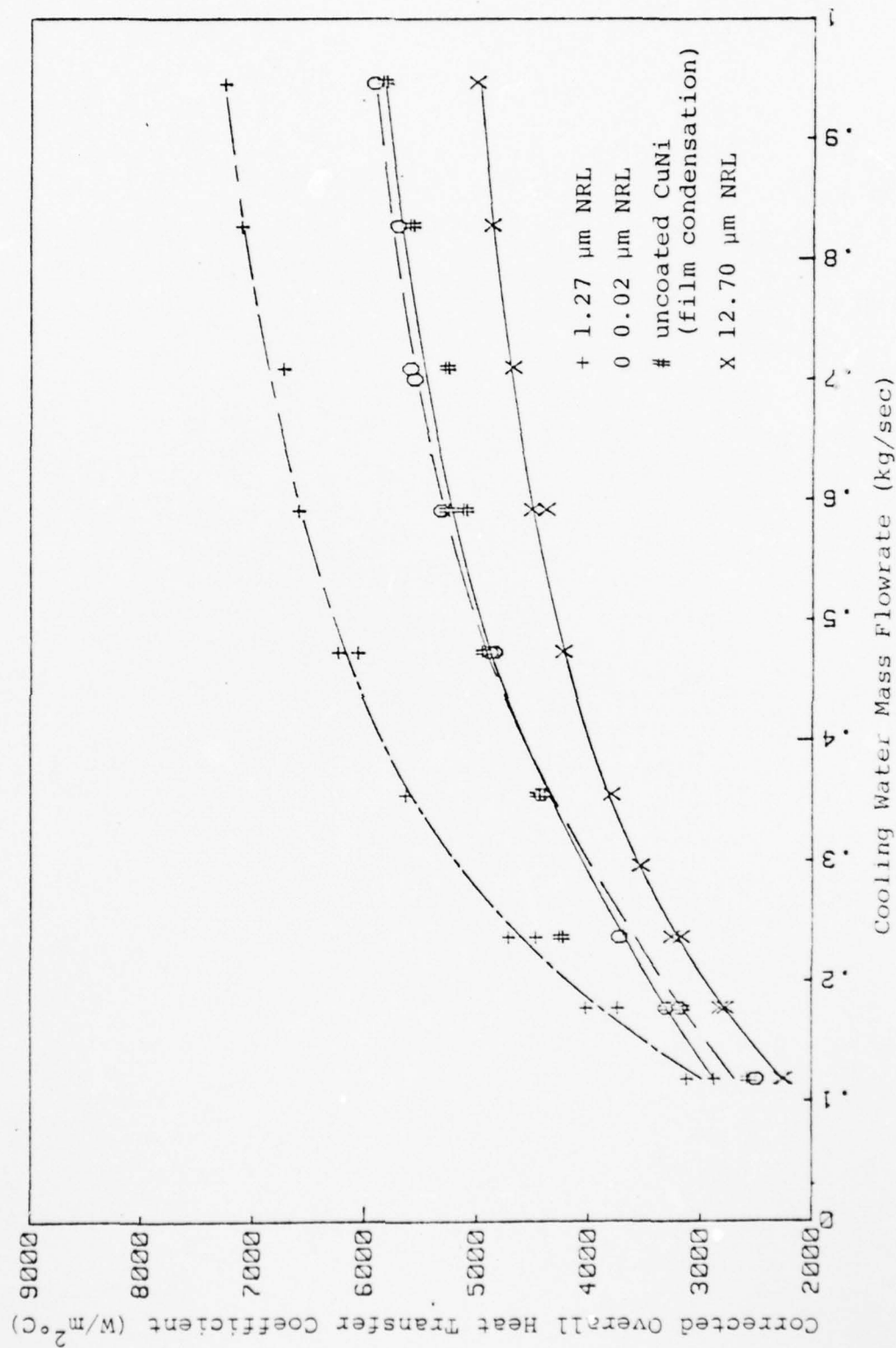


Figure 12. Corrected Overall Heat Coefficient, U_o , versus Cooling Water Mass Flowrate for NRL fluoropoly Coated Tubes.

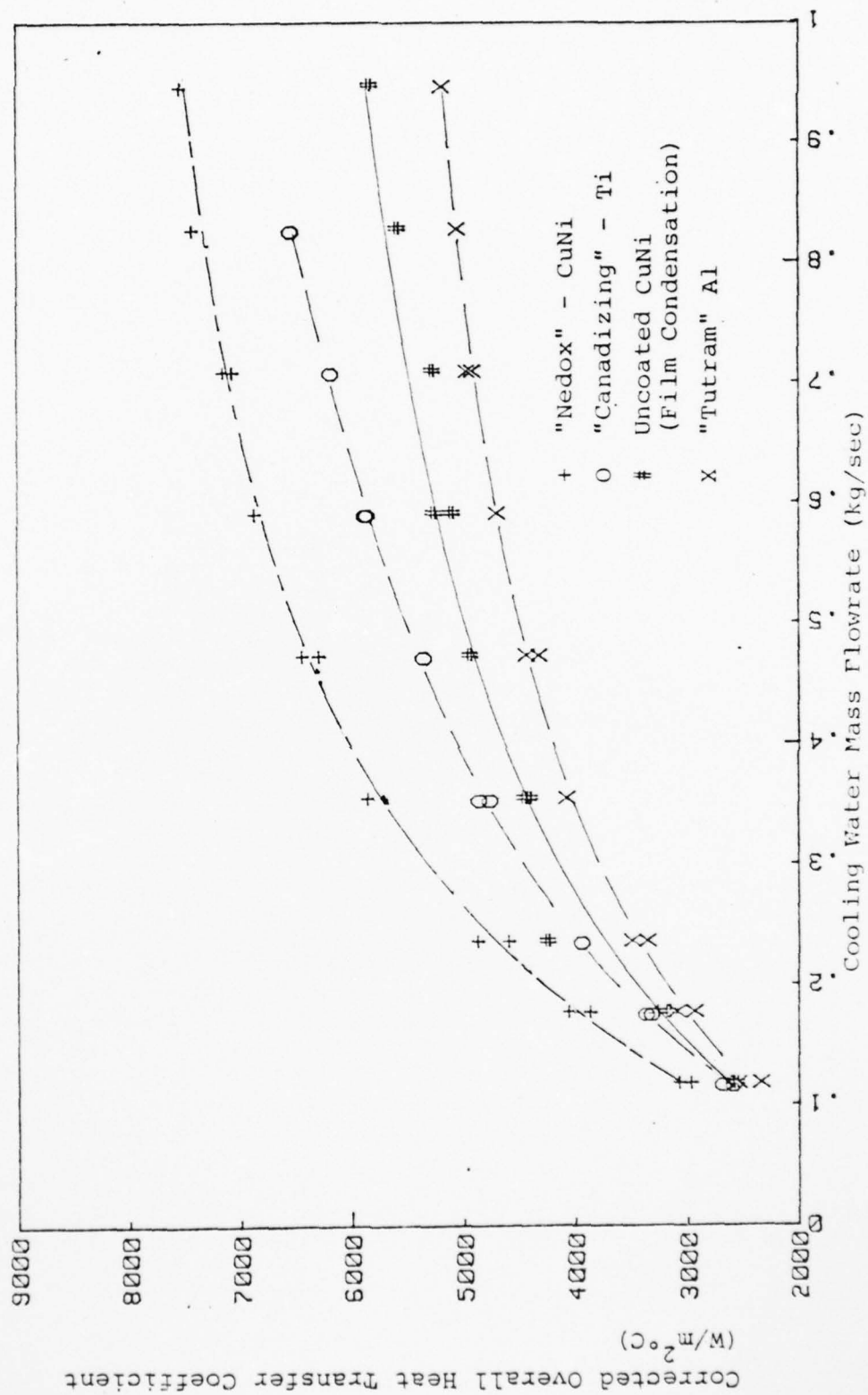


Figure 13. Corrected Overall Heat Transfer Coefficient, U , versus Cooling Water Mass Flowrate for General Magnaplate Corporation Coated Tubes

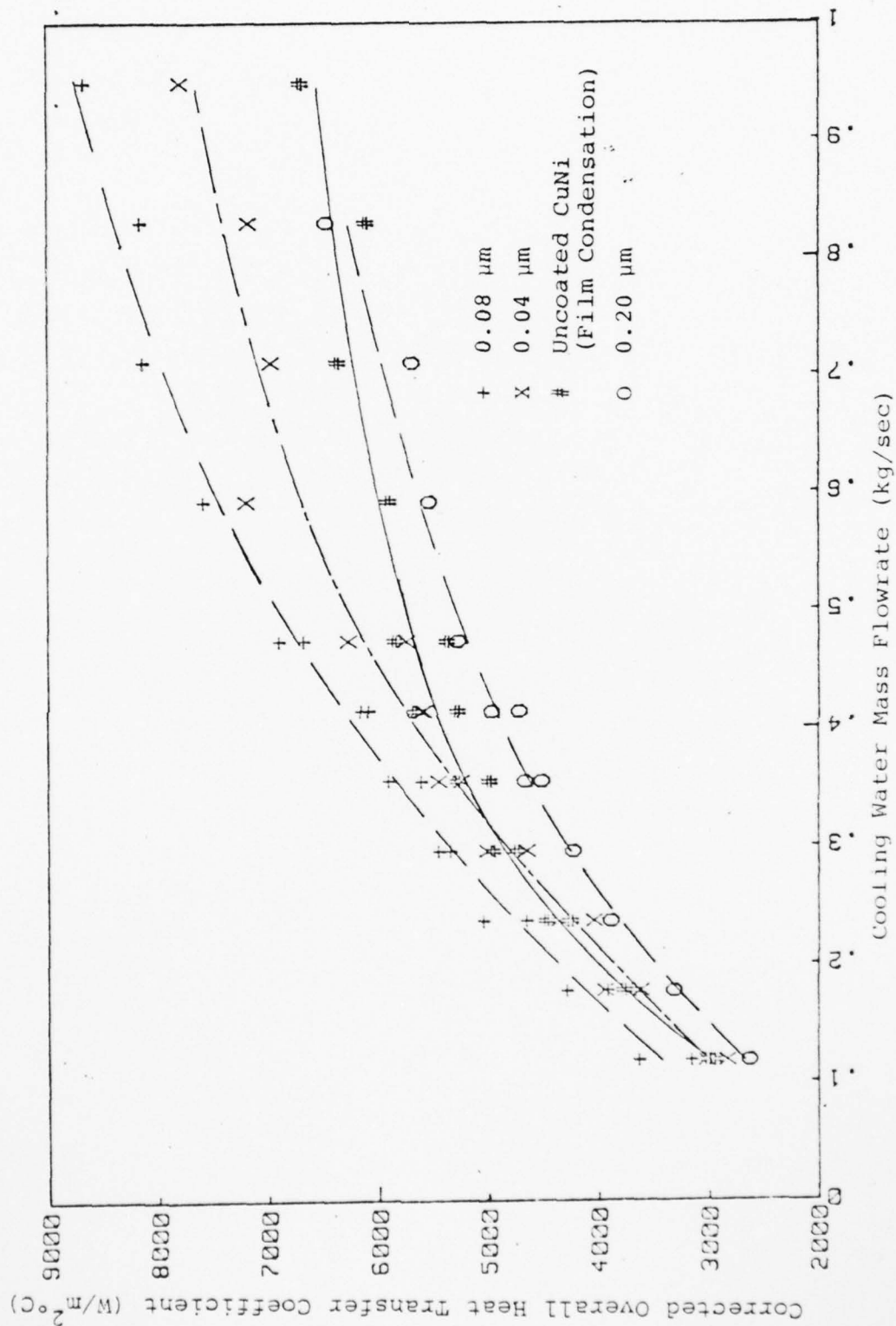


Figure 14. Corrected Overall Heat Transfer Coefficient, U , versus Cooling Water Mass Flowrate for Sputtered TFE Coated CuNi Tubes

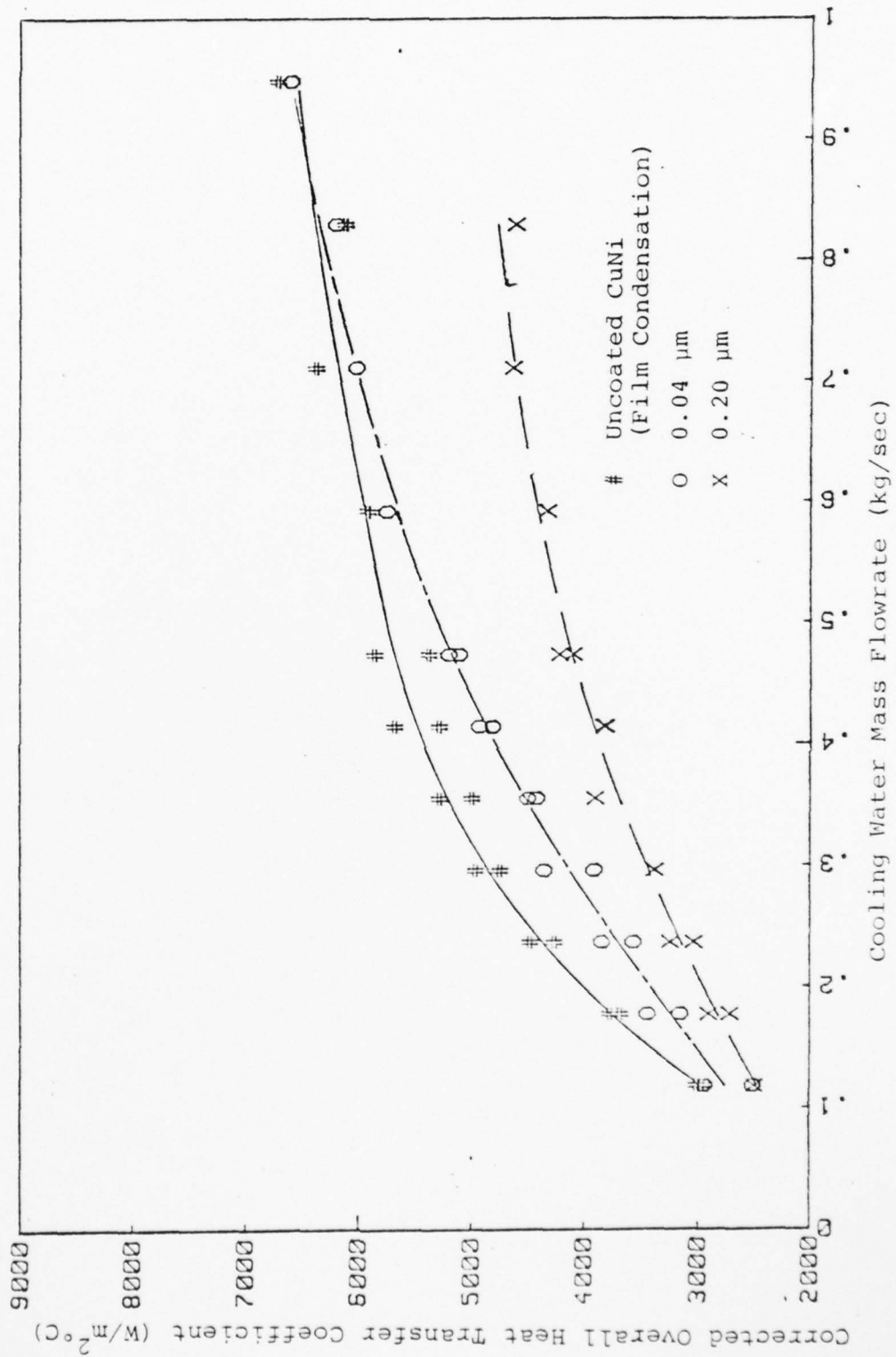


Figure 15. Corrected Overall Heat Transfer Coefficient, U_c , Versus Cooling Water Mass Flowrate for Sputtered TFE Coated Ti Tubes

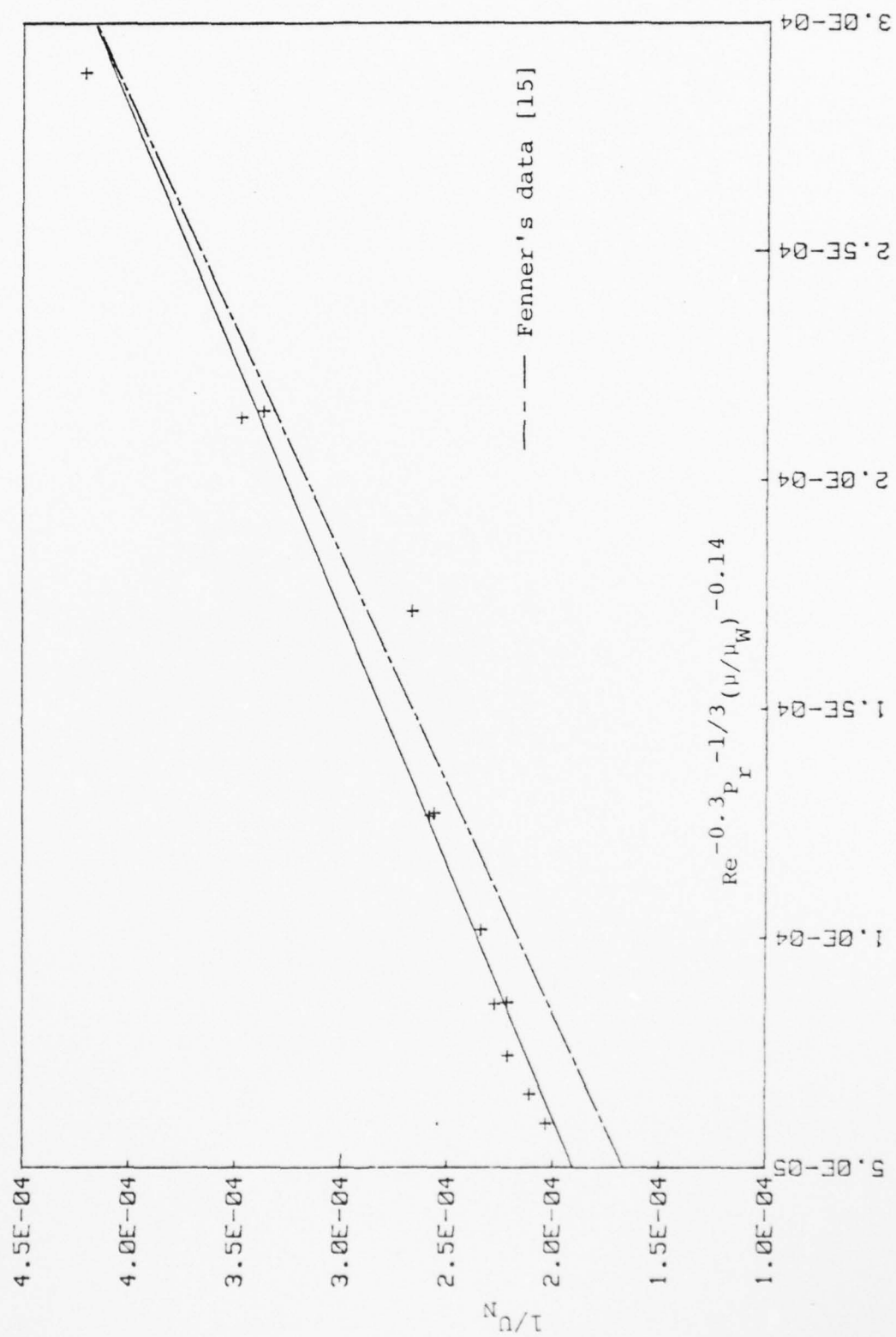


Figure 16. Wilson Plot for Uncoated CuNi (long) Tube

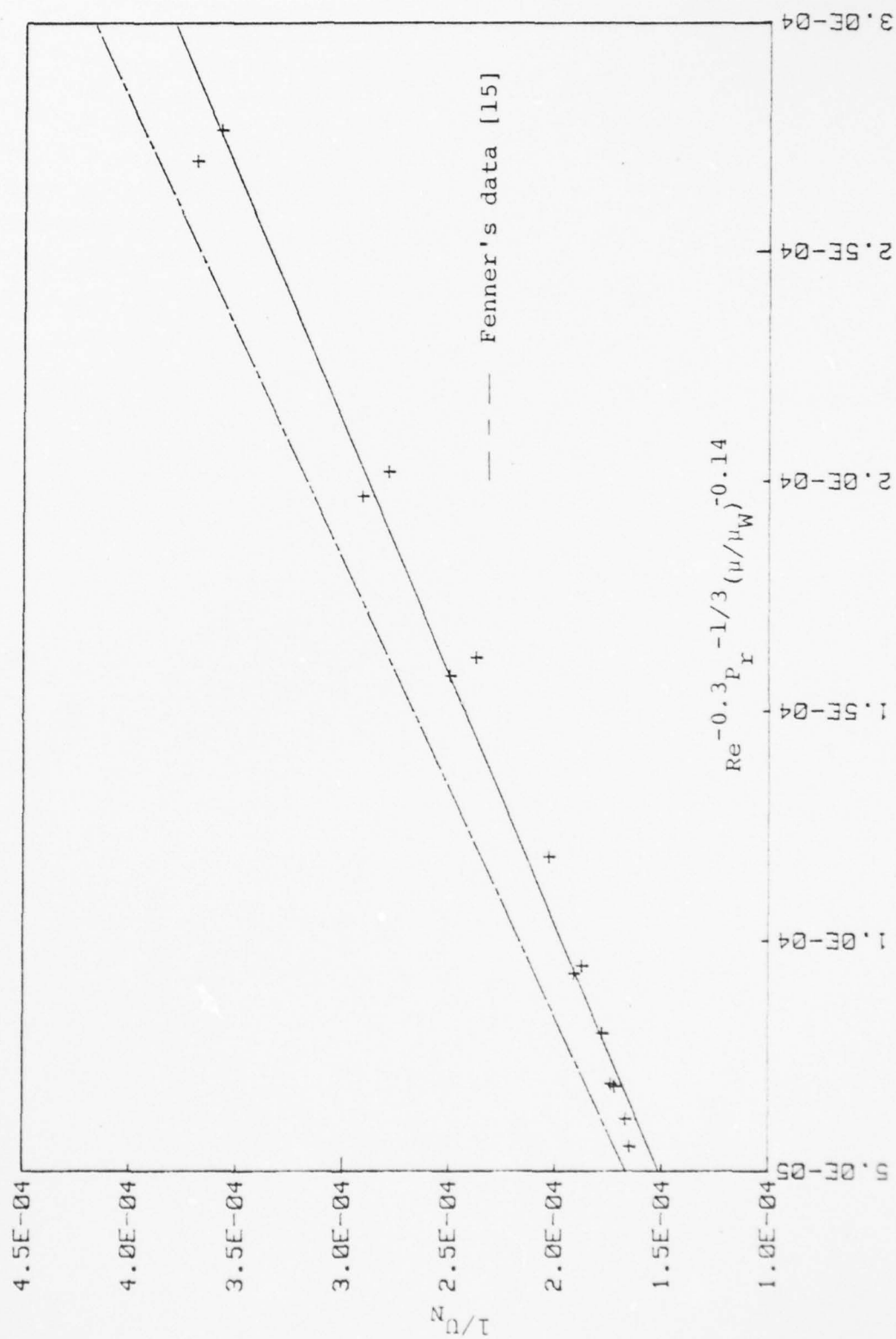


Figure 17. Wilson Plot for "Nedox" Coated CuNi Tube

AD-A072 414

NAVAL POSTGRADUATE SCHOOL MONTEREY CA

F/G 13/10

AN EXPERIMENTAL STUDY OF DROPWISE CONDENSATION ON HORIZONTAL CO--ETC(U)

JUN 79 J T MANVEL

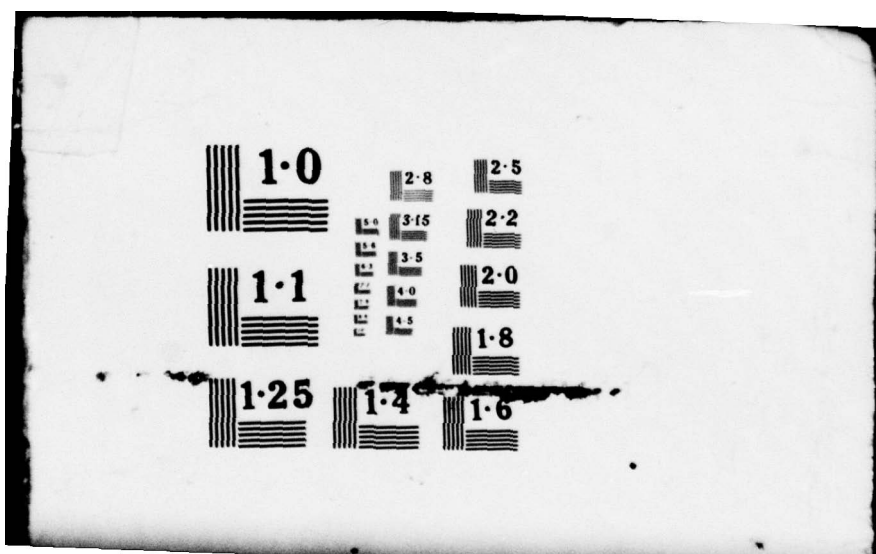
UNCLASSIFIED

NL

2 OF 2
AD
A072414

100

END
DATE
FILMED
9 - 79
DDC



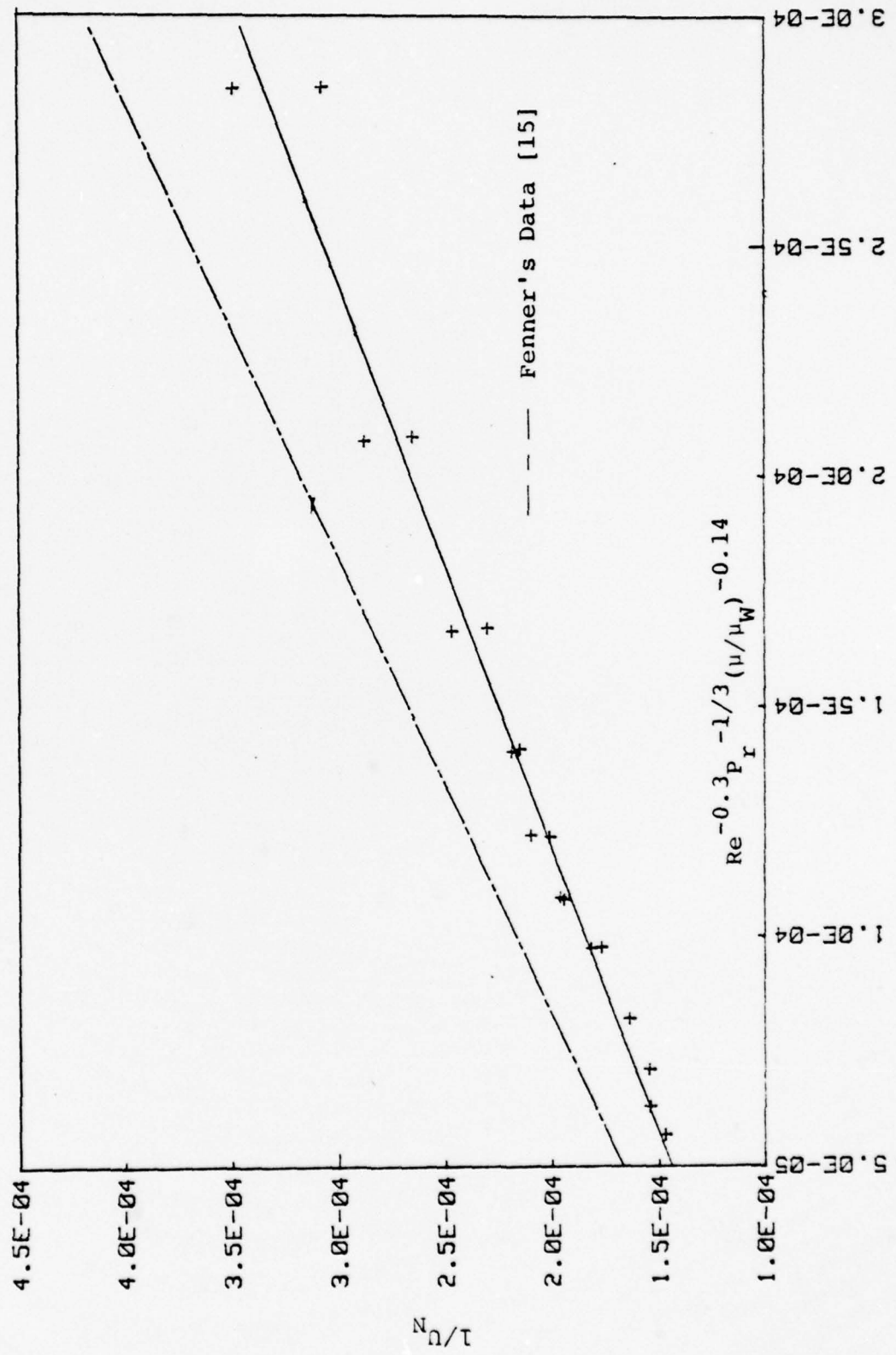


Figure 18. Wilson Plot for Short, 0.08 Sputtered TFE CuNi Tube

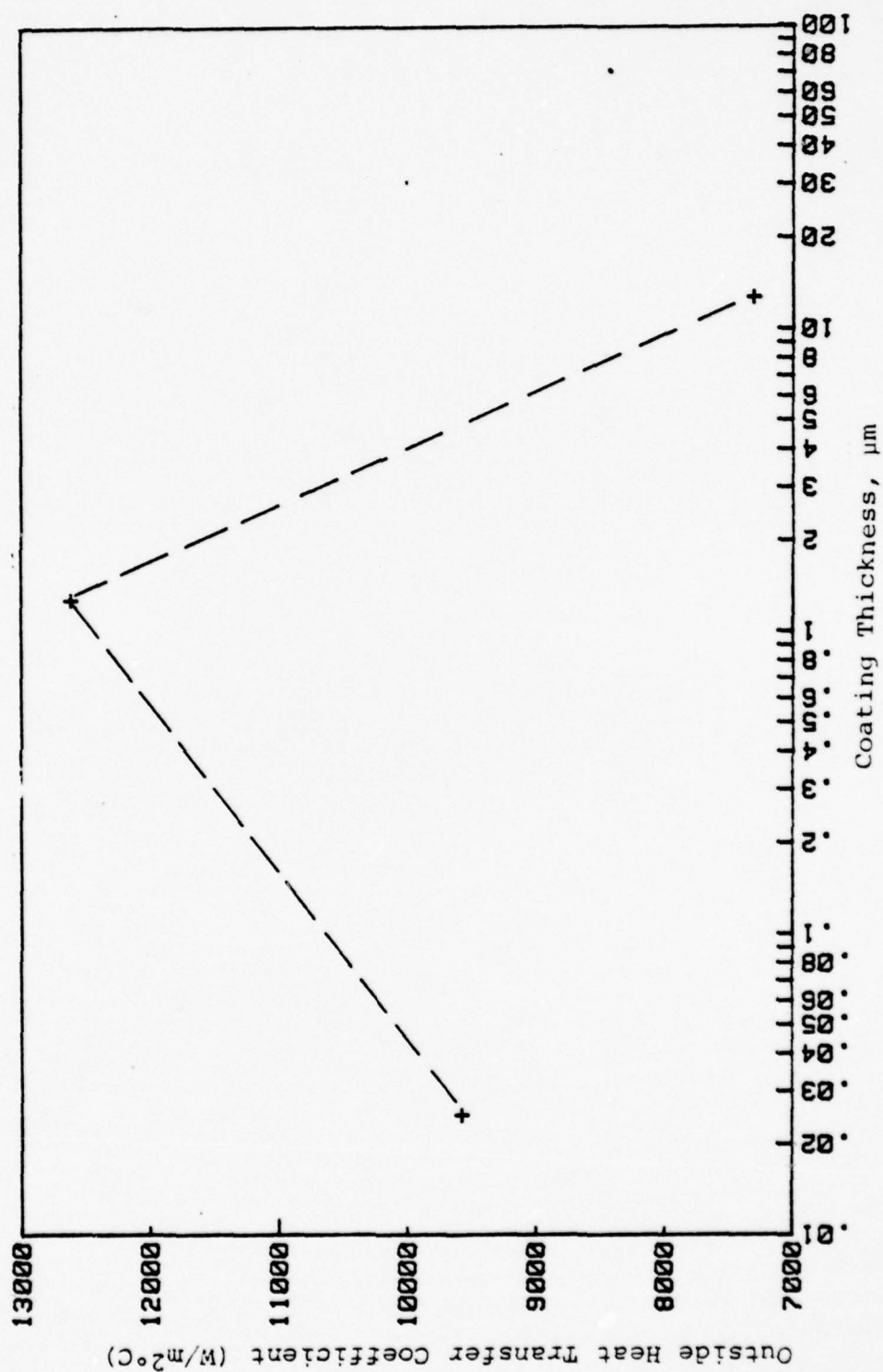


Figure 19. Outside Heat Transfer Coefficient h_o , versus Coating Thickness for NRL Fluoropoly Coated CuNi Tubes

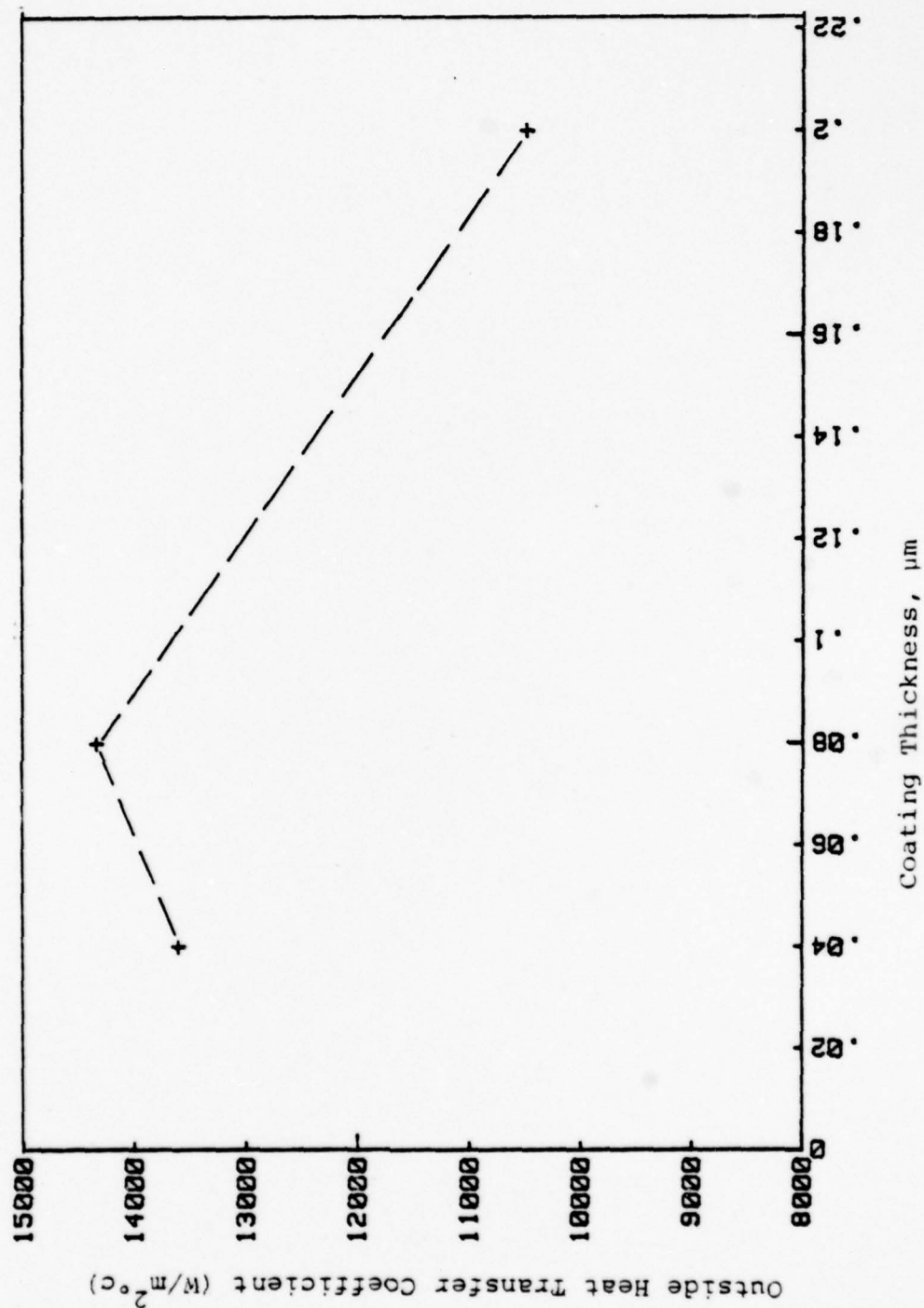


Figure 20. Outside Heat Transfer Coefficient, h_o , versus Coating Thickness for Sputtered TFE Coated CuNi Tubes

APPENDIX A
OPERATING PROCEDURES

I. Light-off Procedures

1. Energize electrical system

- a. In power panel P-2, turn main current breaker to on.
- b. In right side of main control panel, turn key switch on with key.
- c. On left side of main control panel, depress start button of circuit breaker located below the panel of individual circuit breakers.
- d. On left side of main control panel, turn on the circuit breakers for the following equipment.
 - (1) Feed pump
 - (2) Outlets
 - (3) Hot water heater
 - (4) Condensate pump
 - (5) Boiler
 - (6) Cooling tower
 - (7) Cooling water pump.

2. Preheat feedwater

- a. Open sight glass valve and check water level for full feed tank.
- b. Check the following valves for proper alignment for recirculation.

- (1) Sight glass valve - open
 - (2) FW 1 - open
 - (3) Drain valve - close
 - (4) FW 2 - open
 - (5) FW 4 - open
 - (6) DS 2 - open
 - (7) DS 1 - close
- c. On feedwater tank frame, turn on switch to heater element.
 - d. On feedwater tank, turn on heater switch.
 - e. On front of main control panel, turn on feedwater pump.
 - f. Throttle FW 2 to maintain feedwater pump pressure between 5 to 20 psig.
 - g. Check boiler water sight glass to insure that FW 3 is closed.
3. Energize instrumentation
 - a. Multichannel pyrometer.
 - b. Autodata 9 recorder and amplifier.
 - c. Program Autodata using following procedure:
 - (1) Set Time:
 - (a) all alarms and output switches off
 - (b) set date/time on thumbwheels (24 Hour clock)
 - (c) depress the STOP/ENTER switch
 - (d) set the DISPLAY switch to "time"
 - (e) lift the SET TIME switch to enter time.

(2) Assigning Multiple Channels:

- (a) depress the STOP/ENTER switch
- (b) check that all alarms and output switches are still off
- (c) set the SCAN switch to "continuous"
- (d) set the FIRST CHANNEL and LAST CHANNEL thumbwheels to 001
- (e) set the DISPLAY switch to "all" and depress the SLOW switch
- (f) lift the SCAN START switch to start scanning channel 1. To assign channel 1 depress and hold the AUTO and STD RES buttons for at least one scan
- (g) set the LAST CHANNEL thumbwheels to 039 before setting the FIRST CHANNEL thumbwheels to 002
- (h) depress the SKIP button to skip channels 2 through 39 (may have to depress the T/°C button first to break unit out of automode)
- (i) set the LAST CHANNEL thumbwheels to 052 before setting the FIRST CHANNEL thumbwheels to 040
- (j) to assign channels 40 through 52 depress and hold the T/°C and HI RES buttons for at least one complete scan

(3) Interval Scan:

- (a) set thumbwheels to interval desired
between scans (usually one minute)
 - (b) depress the STOP/ENTER switch
 - (c) set the DISPLAY switch to "interval"
 - (d) depress the SET INTERVAL switch
 - (e) set the SCAN switch to "interval"
 - (f) set the FIRST CHANNEL thumbwheels to
001
 - (g) set the LAST CHANNEL thumbwheels to
052
 - (h) lift the SCAN START switch
- (4) Use the following as needed/desired:
- (a) printer on/off
 - (b) SLOW switch
 - (c) single channel display

4. Raise vacuum in condenser

a. Align valves to the following settings:

- (1) Cold trap draw valve - close
- (2) Cold trap inlet valve - open
- (3) Upper hot well draw valve - open
- (4) MS-5 - open
- (5) MS-6 - open
- (6) Desuperheater drain tank draw valve - closed
- (7) MS-4 - close
- (8) MS-3 - close

- (9) MS-2 - close
 - (10) C-2 - close
 - (11) MS-1 - close
 - (12) Main steam separator drain valve - close
 - b. Turn on cold trap refrigeration unit.
 - c. Turn on vacuum pump.
 - d. Regulate vacuum as necessary with bleed valve.
5. Once vacuum is assured, and feedwater temperature has reached 60°C, energize boiler.
6. Cooling Water System
- a. Open valve CW-1; then open valve CW-2 one turn to prime the cooling water pump, keeping valves SW-3 and CW-4 closed.
 - b. Energize cooling water pump (switch near pump), and close valve CW-2. Open valve CW-3 one turn until flow is established, then open valve CW-4 to purge air.
 - c. Open valves CW-3 and CW-4 to obtain desired flow rates.
 - d. Vent both sides of the 3.66 meter manometer.
 - e. When using the house water supply remove plug from sump and open valve CW-2 with valve CW-1 closed. Follow step 3.
 - f. Begin flow to secondary condenser (valve behind column next to boiler).

7. Steam System

a. Boiler Operation

- (1) When boiler has reached the desired pressure (approximately 20.7 kPa) open valve MS-1.
- (2) Insure valves MS-6 and MS-5 are open.
- (3) Open valve MS-3 to obtain desired steam flow rate to test condenser. Open valve MS-4 as necessary to maintain boiler pressure at desired level (34.5 kPa).

b. House Steam

- (1) Insure valve MS-1 is closed. Open valve MS-2.
- (2) Follow steps (b) and (c) for boiler use.

8. Condensate and Feedwater System

a. Using Boiler

- (1) To collect drains in test condenser hotwell operate with valve C-1 closed. After test run has been completed, open valve and condensate will drain into secondary condenser.
- (2) The condensate pump is operated intermittently, when level in secondary condenser dictates. When pump is secured, keep valve C-2 closed. When pump is required, start pump and then open valve C-2. In this mode keep valve C-3 closed.
- (3) While feed pump is running (continuous operation) valve FW-1 must be fully open and valve FW-2

must be throttled so that a positive flow is insured. Valve FW-3 is a solenoid valve which is actuated by the boiler controls.

- (4) When boiler is energized, valve FW-4 must be fully open.
- (5) Make-up is added to the system through the top of the feedwater tank by removing anode.

II. Securing Procedures

1. Using Boiler

- a. Close valves MS-3 and MS-4. Secure power to boiler and then close MS-1.
- b. Close valve DS-1 and drain desuperheater hotwell.
- c. Pump condensate from secondary condenser hotwell to feedwater tank. Secure valve C-2.
- d. Secure vacuum pump and refrigeration unit.
- e. Secure power to heater (switches on side and stand).
- f. Secure flow to secondary condenser.
- g. Bottom blow boiler to remove deposits. Repeat twice, blowing from high water mark to low water mark each time.
- h. Secure cooling water pump or close valve CW-2 when using house water supply. Close valves CW-3 and CW-4.
- i. Secure instrumentation.
- j. Secure power to feed pump.

- k. De-energize individual circuit breakers.
- l. De-energize circuit breaker on control panel;
depress stop button. Turn key switch off.

III. Secondary Systems

1. Vacuum System

Vacuum is established by a mechanical vacuum pump and is controlled by a vacuum regulator mounted on instrument board mounted by test condenser. The vacuum pump is separated from the condenser system by a refrigerated cold trap to prevent moisture from entering the pump.

2. Desuperheater

Valve DS-1 controls flow of feedwater (60°C) to spray nozzles. Optimum flow level is between 15 and 20 percent flow on rotameter. Condensate is collected in a small tank below desuperheater so the mass flow rate can be determined.

IV. Safety Devices

1. Emergency Power Shut-Off

To secure all power to the system in an emergency, depress the red button on the right of the main control panel next to the key switch.

2. Boiler

- a. The mercury switches mounted on the main control panel secure power to the heating elements of

the boiler when the steam pressure exceeds 172.4 kPa. Power is restored to the heating elements when the pressure drops to approximately 103.4 kPa.

- b. A low water level limit switch is contained within the boiler, and when the water level inside the boiler drops below a preset level, power is secured to the boiler and will not be restored until the water level is above this preset height.
- c. The relief valve mounted on the boiler is set to lift at 206.8 kPa.

APPENDIX B

SAMPLE CALCULATIONS

A sample calculation is performed to illustrate how the data reduction program progresses to the results for the 0.20 micron sputtered TFE coated 90-10 copper-nickel tube, at 15 percent flow. This run is the same used for the error analysis in Appendix C, and for the temperature adjustment subroutine in Appendix D.

INPUT PARAMETERS

Tube	90-10 copper-nickel, Tube M		
Coating	Sputtered TFE, 0.20 micron thick		
Tube Inside Diameter (D_i)	0.013157 m		
Tube Outside Diameter (D_o)	0.015875 m		
Overall Tube Length (L)	0.1524 m		
Cross Section Flow Area (AC)	0.0001354 m ²		
Outside Nominal Surface Area (A_N)	0.0076006 m ²		
Tube Thermal Conductivity (K_w)	44.652 W/m°C		
Wall Resistance, R_w	3.37232 (10 ⁻⁵) m ² °C/W		
Cooling Water Inlet Temperature (TC_L)	14.92°C		
Cooling Water Outlet Temperature (TC_O)	17.26°C		
Average Cooling Water Temperature (TB,TBR)	16.09°C	289.24°K	
	60.96°F	520.63°R	
Steam Vapor Temperature (T_v)	67.77°C		

Tube Wall Temperature (T_w) 43.71°C = 316.36°K

Tube Pressure Drop (ΔP_m) 2.6668 kPa

% Flow (100% = 71.2 l/m) 15%

A. CALCULATIONS OF COOLING WATER PROPERTIES

1. Determination of Dynamic Viscosity WMHU(I)^{*} = μ

$$\mu = \frac{1}{2419.2} \exp[(4.606532 \times 10^{-3})(TBR) + \frac{4759.5941}{TBR} - 10.59252566]$$

$$\mu = \frac{1}{2419.2} \exp[(4.606532 \times 10^{-3})(520.63) + \frac{4759.5941}{520.63} - 10.59252566]$$

$$\mu = \underline{1.0664398 \times 10^{-3} \text{ Kg/m}\cdot\text{sec}}$$

2. Determination of Thermal Conductivity, $H_{20K} = K$

$$K = 0.59303069 + 1.9248784 \times 10^{-3} TB - 7.0238534 \times 10^{-6} TB^2 - 2.0913612 \times 10^{-10} TB^3$$

$$K = 0.59303069 + 1.9248784 \times 10^{-3} (16.09) - 7.0238534 \times 10^{-6} (16.09)^2 - 2.0913612 \times 10^{-10} (16.09)^3$$

$$K = \underline{0.62218033 \text{ W/m}^\circ\text{C}}$$

3. Determination of Density, $\text{RHO(I)} = \rho$

$$\rho = 1001.434664 - 0.21175821 \text{ TB} - 2.3913147 \times 10^{-3} \text{ TB}^2$$

$$\rho = 1001.434664 - 0.21175821(16.09) - 2.3913147 \times 10^{-3}(16.09)^2$$

$$\underline{\rho = 997.4087123 \text{ Kg/m}^3}$$

4. Determination of Specific Heat, $\text{CP(I)} = c_p$

$$c_p = 4.2092198 - 1.3594085 \times 10^{-3} \text{ TB} + 1.3948397 \times 10^{-5} \text{ TB}^2$$

$$c_p = 4.2092198 - 1.3594085 \times 10^{-3}(16.09) + 1.3948397 \times 10^{-5}(16.09)^2$$

$$\underline{c_p = 4.1909590 \text{ KJ/Kg}^\circ\text{C}}$$

5. Determination of Dynamic Viscosity at inside of Tube Wall, $\text{WALMH} = \mu_W$

$$\mu_W = \exp[4.606532 \times 10^{-3} (\text{TW}^\circ\text{R}) + \frac{4759.5941}{(\text{TW}^\circ\text{R})} - 10.59252566]$$

$$\mu_W = \exp[4.606532 \times 10^{-3}(570.35) + \frac{4759.5941}{570.35} - 10.59252566]$$

$$\mu_W = 1.4620664 \text{ lbm/ft hr}$$

$$\mu_W = \left(\frac{1 \text{ Kg/meter-sec}}{2419.2 \text{ lbm/ft hr}} \right) (1.4620664 \text{ lbm/ft hr})$$

$$\underline{\mu_W = 6.0435947 \times 10^{-4} \text{ Kg/m} \cdot \text{sec}}$$

6. Determination of Mass Flowrate, DOTM = \dot{m}

$$\dot{m} = (\% \text{ Flow}) (71.2 \text{ liter/min}) \left(\frac{\text{m}^3}{1000 \text{ liter}} \right) \left(60 \frac{\text{min}}{\text{hr}} \right)$$

$$\dot{m} = \frac{(997.4087123) (.15) (71.2) (60)}{1000}$$

$$\dot{m} = \underline{639.1395025 \text{ Kg/hr}} = 0.177538751 \text{ Kg/sec}$$

7. Determination of Velocity, $V(I) = v$

$$v = \frac{4 \dot{m}}{D_i^2}$$

$$v = \frac{(4) (0.177538751)}{(\pi) (997.4087123) (0.013157)}$$

$$\underline{v = 1.3092 \text{ meter/sec}}$$

8. Determination of Prandtl Number

$$P_r = \frac{\mu C_p}{k} = \frac{(1.06654 \times 10^{-3})(4.1909590)}{(0.62218083)}$$

$$\underline{P_r = 7.18345}$$

9. Determination of the Reynolds Number

$$Re = \frac{\rho V D_i}{\mu}$$

$$Re = \frac{(997.4087123)(1.3092)(0.0131572)}{(1.06654 \times 10^{-3})}$$

$$\underline{Re = 16,102.3}$$

B. CONDENSATE FILM PROPERTIES CALCULATIONS IN TEMPERATURE ADJUSTMENT SUBROUTINE, TADJ.

1. Determination of Film Temperature, $T_F = T_f$

$$T_f = (T_W + T_V)/2$$

$$T_f = (43.71 + 67.77)/2$$

$$T_f = 55.74^\circ\text{C}$$

2. Determination of Density, $D_{FLM} = \rho_f$

$$\rho_f = 1003.322147 - 1.7285196 \times 10^{-1} T_f - 2.7879777 \times 10^{-3} T_f^2$$

$$\rho_f = 1003.322147 - 1.7285196 \times 10^{-1} (55.74^\circ\text{C}) \\ - 2.7879777 \times 10^{-3} (55.74)^2$$

$$\rho_f = \underline{985.0244721 \text{ Kg/m}^3}$$

3. Determination of Enthalpy, HFG = H_{fg}

$$H_{fg} = 2.3765503 \times 10^3 - 2.3647321 T_V + 3.2767270 \times 10^{-4} T_V^2 \\ - 1.1969960 \times 10^{-5} T_V^3$$

$$H_{fg} = \underline{2214.0661 \text{ KJ/Kg}}$$

4. Determination of Film Conductivity, CFLM = K_f

$$K_f = 0.563407054 - 2.0082260 \times 10^{-3} T_f - 8.2609779 \times 10^{-6} T_f^2$$

$$K_f = 0.563407054 + 2.0082260 \times 10^{-3} (55.74) \\ - 8.260977 \times 10^{-6} (55.74)^2$$

$$K_f = \underline{0.649680961 \text{ W/m}^\circ\text{C}}$$

5. Determination of Film Dynamic Viscosity, VFLM = μ_f

$$\mu_f = 1.4717837 \times 10^{-3} - 2.9273525 \times 10^{-5} T_f \\ + 2.5915293 \times 10^{-7} T_f^2 - 8.4752236 \times 10^{-10} T_f^3$$

$$\mu_f = 1.4717837 \times 10^{-3} - 2.9273525 \times 10^{-5} (55.74)$$

$$+ 2.5915293 \times 10^{-7} (55.74)^2 - 8.4752236 \times 10^{-10} (55.74)^3$$

$$\mu_f = 4.9846320 \times 10^{-4} \text{ Kg/m}\cdot\text{sec}$$

C. CALCULATION OF THE TEMPERATURE ADJUSTMENT FOR SHORT TUBE

1. Determination of Filmwise Heat Transfer Coefficient on Bare Tube Extensions (GADZ)

$$h_o = 0.725 \left[\frac{\rho_f^2 g h_{fg} K_f^3}{\mu_f D_o (T_V - T_W)} \right]^{0.25}$$

$$h_o = 0.725 \left[\frac{(985.0244721)^2 (9.805) (2.214066 \times 10^6) (0.649680961)^3}{(4.9846320 \times 10^{-4}) (0.015875) (67.77 - 43.71)} \right]^{0.25}$$

$$h_o = 9568.317 \text{ W/m}^2\text{C}$$

2. Determination of Inside Heat Transfer Coefficient on Inside of Tube Extensions

$$h_i = \frac{0.023K}{D_i} \text{Re}^{0.8} \text{Pr}^{0.4}$$

$$h_i = \frac{0.023}{0.013132} (0.62218083) (16102.291)^{0.8} (7.18345)^{0.4}$$

$$\underline{h_i = 5563.614 \text{ W/m}^2\text{C}}$$

3. Determination of Heat Flux through the gap between insulation and tube wall, GAP1

$$\frac{Q_{\text{gap}}}{L} = \left(\frac{T_V - T_B}{\frac{1}{\pi D_i h_i} + \frac{\ln(D_o/D_i)}{2\pi K} + \frac{1}{\pi D_o h_o}} \right)$$

$$\frac{1}{\pi D_i h_i} = \frac{1}{(\pi)(0.0131572)(5563.614)}$$

$$= 4.3567462 \times 10^{-3} \text{ } ^\circ\text{C/Wm}$$

$$\frac{\ln(D_o/D_i)}{2\pi K} = \frac{\ln(0.015875)(0.0131572)}{(2)(\pi)(41.652.06)}$$

$$= 0.669298 \times 10^{-3} \text{ m}^\circ\text{C/W}$$

$$\frac{1}{\pi D_o h_o} = \frac{1}{(\pi)(0.015875)(0568.317)} = 2.0975507 \times 10^{-3} \text{ m}^\circ\text{C/W}$$

$$\frac{Q_{\text{gap}}}{L} = \frac{(67.77 \text{ } 0 \text{ } 16.09)^\circ\text{C}}{7.123595 \times 10^{-3} \text{ m}^\circ\text{C/W}} = 7255.232 \text{ W/m}$$

$$\text{GAP}_2 = .0762 \text{ m}$$

$$Q_{\text{GAP}} = (.0762\text{m})(7255.232 \text{ W/m}) = \underline{552.849 \text{ W's}}$$

4. Determination of Heat Flux through the Insulated Tube Extensions, Q_{IN}

$$\frac{Q_{IN}}{L_{IN}} = \left(\frac{T_V - T_B}{\frac{1}{2\pi K_{ext}} \ln\left(\frac{D_o}{D_i}\right) + \frac{1}{2\pi K_{IN}} \ln\left(\frac{D_o + 2t_{IN}}{D_o}\right)} \right)$$

$$R_{ext} = \frac{1}{2\pi K_{ext}} \ln\left(\frac{D_o}{D_i}\right)$$

$$R_{ext} = \frac{\ln(0.015875/0.0131572)}{2\pi(16.26858)} = 1.8370100 \times 10^{-3} \text{ m}^\circ\text{C/W}$$

$$R_{IN} = \frac{\ln[(0.015875 + 2(4.7625 \times 10^{-3})/0.015875)}{2\pi(1.4659 \times 10^{-1})}$$

$$R_{IN} = 0.510288 \times 10^{-3} \text{ m}^\circ\text{C/W}$$

$$\frac{Q_{IN}}{L_{IN}} = \left(\frac{67.77 - 16.09}{0.51212694} \right) = 100.919 \text{ W/m}$$

$$L_{IN} = 0.7239 \text{ m}$$

$$Q_{IN} = (100.919)(0.7239) = \underline{73.055 \text{ W}}$$

5. Determination of Undesired Heat Flux, Q_{error}

$$\begin{aligned} Q_{error} &= Q_{IN} + Q_{gap} = 73.055 + 552.849 \\ &= \underline{625.904 \text{ W}} \end{aligned}$$

Determination of Measured Heat Flux, Q_m

$$\begin{aligned} Q_m &= \dot{m} c_p (T_{c_o} - T_{c_i}) \\ &= (0.177538751) (4190.959) (17.26 - 14.92) \end{aligned}$$

$$\underline{Q_m = 1740.268 \text{ W}}$$

Determination of Correct Heat Flux through Test Tube

$$\begin{aligned} Q_{\text{CORR}} &= Q_m - Q_{\text{error}} = 1740.268 - 625.904 \\ &= 1114.364 \text{ W} \end{aligned}$$

6. Determination of Correct Temperature Difference Across Test Tube

$$\begin{aligned} \Delta T_{\text{CORR}} &= \frac{Q_{\text{CORR}}}{\dot{m} c_p} = \frac{1114.364}{(0.177538751) (4190.959)} \\ &= 1.49^\circ\text{C} \end{aligned}$$

7. Determination of Temperature Adjustments

$$T_{\text{adj}} = \frac{\Delta T_m - \Delta T_{\text{CORR}}}{2} = \frac{2.34 - 1.58}{2} = 0.38^\circ\text{C}$$

8. Determination of Adjusted Cooling Water Inlet Temperature $T_{c_i}^*$, and Outlet Temperature, $T_{c_o}^*$

$$T_{c_i}^* = T_{c_i} + T_{adj} = 14.92 + 0.38 = 15.30^\circ\text{C}$$

$$T_{c_o}^* = T_{c_o} + T_{adj} = 17.26 - 0.38 = 16.88^\circ\text{C}$$

D. CALCULATIONS OF CHARACTERISTIC HEAT TRANSFER PARAMETER

1. Determination of Overall Heat Transfer Coefficient

$$\begin{aligned} U_N &= \frac{\dot{m} c_p}{A_N} \ln \frac{(T_V - T_{c_i}^*)}{(T_V - T_{c_o}^*)} \\ &= \frac{(0.177538751)(4190.959)}{(0.0076006)} \ln \frac{(67.77 - 15.30)}{(67.77 - 16.88)} \\ &= \underline{2996.879 \text{ W/m}^2\text{C}} \end{aligned}$$

2. Determination of Corrected Overall Heat Transfer Coefficient, U_c

$$\begin{aligned} U_c &= \frac{1}{\frac{1}{U_N} - R_W} = \frac{1}{\frac{1}{2996.879} - 3.37232 \times 10^{-5}} \\ &= \underline{3318.624 \text{ W/m}^2\text{C}} \end{aligned}$$

3. Determination of Wilson Plot Parameters

- (a) Abscissa

$$X = \frac{1}{Re^{0.8} P_r^{0.33} \left(\frac{\mu}{\mu_N}\right)^{0.14}}$$

$$X = \frac{1}{(16102.291)^{0.8} (7.18345)^{0.33} \left(\frac{1.00665 \times 10^{-3}}{6.0435947 \times 10^{-4}} \right)^{0.4}}$$

$$X = \underline{2.076 \times 10^{-4}}$$

(b) Ordinate

$$Y = \frac{1}{U_N} = \frac{1}{2996.879} = \underline{3.3368047 \times 10^{-4}}$$

4. Determination of Sieder-Tate Constant

$$C_i = \frac{D_o}{M K_b} = \frac{1.5875 \times 10^{-2}}{(0.91755)(0.62218083)} = 0.0257$$

5. Determination of Inside Heat Transfer Coefficient, HI = h_i

$$\begin{aligned} h_i &= \frac{C_i K}{D_i} \text{Re}^{0.8} \text{Pr}^{1/3} \left(\frac{\mu}{\mu_N} \right)^{0.14} \\ &= \frac{(2.572517 \times 10^{-2})(0.62218083)(16102.291)^{0.8} (7.18345)^{0.33}}{(0.0131572)} \\ &\quad \times \left(\frac{1.0664398 \times 10^{-3}}{6.0435947 \times 10^{-4}} \right)^{0.14} \end{aligned}$$

$$h_i = \underline{5896.980 \text{ W/m}^2\text{°C}}$$

6. Determination of Outside Heat Transfer Coefficient,
 $H_o = h_o$

$$\begin{aligned}
 h_o &= \frac{1}{\frac{1}{U_N} - R_W - \frac{D_o}{D_i h_i}} \\
 &= \frac{1}{\frac{1}{2996.879} - 3.3732 \times 10^{-5} - \frac{(0.015875)}{(0.0131572)(5806.98)}} \\
 &= \underline{10338.836 \text{ W/m}^2\text{°C}}
 \end{aligned}$$

APPENDIX C

UNCERTAINTY ANALYSIS

The basic equations used in this section are reproduced from Reilly [16]. The general form of the Kline and McClintock [28] "second order" equation is used to compute the probable error in the results. For some resultant, R , which is a function of summary variables X_1, X_2, \dots, X_n the probable error in R , δR is given by

$$\delta R = \left[\left(\frac{\delta R}{\delta X_1} \delta X_1 \right)^2 + \left(\frac{\delta R}{\delta X_2} \delta X_2 \right)^2 + \dots + \left(\frac{\delta R}{\delta X_n} \delta X_n \right)^2 \right]^{1/2} \quad (C-1)$$

where $\delta X_1, \delta X_2, \dots, \delta X_n$ are the probable errors in each of the measured variables.

C.1. Uncertainty in Overall Heat Transfer Coefficient, U_N

The overall heat transfer coefficient is given by equation (4), in Chapter III as

$$U_N = \frac{\dot{m} c_p}{A_N} \ln \left[\frac{T_V - T_{c_i}}{T_V - T_{c_o}} \right] \quad (4)$$

By applying equation (C-1) to equation (4) the following equation results:

$$\frac{\delta U_n}{U_n} = \left[\left(\frac{\delta A_n}{A_n} \right)^2 + \left(\frac{\delta c_p}{c_p} \right)^2 + \left(\frac{\delta \dot{m}}{\dot{m}} \right)^2 + \left(\frac{\delta T_v (T_{c_i} - T_{c_o})}{(T_v - T_{c_i})(T_v - T_{c_o}) \ln \frac{T_v - T_{c_i}}{T_v - T_{c_o}}} \right)^2 \right. \\ \left. + \left(\frac{\delta T_{c_i}}{(T_v - T_{c_i}) \ln \frac{T_v - T_{c_i}}{T_v - T_{c_o}}} \right)^2 + \left(\frac{\delta T_{c_o}}{(T_v - T_{c_o}) \ln \frac{T_v - T_{c_i}}{T_v - T_{c_o}}} \right)^2 \right]^{1/2} \quad (C-2)$$

The following are the values assigned to the variables:

$$\delta c_p = 0.0042 \text{ KJ/Kg}^\circ\text{C}$$

$$\delta \dot{m} = 0.01 \dot{m} \text{ Kg/sec}$$

$$\delta T_v = 1.0^\circ\text{C}$$

$$\delta T_{c_o} = 0.2^\circ\text{C}$$

$$\delta T_{c_i} = 0.2^\circ\text{C}$$

$$\delta A_N = 9.29 \times 10^{-5} \text{ m}^2$$

$$\frac{\delta U_N}{U_N} = \left[\left(\frac{9.29 \times 10^{-5}}{7.6006 \times 10^{-3}} \right)^2 + \left(\frac{.0042}{4.19096} \right)^2 + \left(\frac{.01 \dot{m}}{1 \dot{m}} \right)^2 \right. \\ \left. + \left(\frac{(1.0)(-1.58)}{(52.47)(50.39) \ln(1.031)} \right)^2 + \left(\frac{0.2}{52.47 \ln(1.031)} \right)^2 \right. \\ \left. + \left(\frac{0.2}{50.89 \ln(1.031)} \right)^2 \right]^{1/2}$$

$$\frac{\delta U_N}{U_N} = 0.18$$

$$\underline{U_{N,15\%} = 2997 \pm 539 \text{ W/m}^2 \text{ } ^\circ\text{C}}$$

C.2. Uncertainty in Inside Heat Transfer Coefficient, h_i

The probable error in the inside heat transfer coefficient is given by:

$$\begin{aligned} \frac{\delta h_i}{h_i} = & \left[\left(\frac{\delta k}{k} \right)^2 + \left(\frac{\delta D_i}{D_i} \right)^2 + \left(\frac{0.8 \delta Re}{Re} \right)^2 + \left(\frac{0.333 \delta Pr}{Pr} \right)^2 \right. \\ & \left. + \left(\frac{\delta C_i}{C_i} \right)^2 + \left(\frac{0.14 \delta (\mu/\mu_w)}{\mu/\mu_w} \right)^2 \right]^{1/2}, \end{aligned} \quad (C-3)$$

where:

$$\delta k = 0.030 \text{ W/m } ^\circ\text{C},$$

$$\delta D_i = 0.00051 \text{ m},$$

$$\delta Pr = 0.10, \text{ and}$$

$$\delta \left(\frac{\mu}{\mu_w} \right) = 0.050.$$

The probable error in the Reynolds number is given by:

$$\frac{\delta Re}{Re} = \left[\left(\frac{\delta G}{G} \right)^2 + \left(\frac{\delta \mu}{\mu} \right)^2 + \left(\frac{\delta D_i}{D_i} \right)^2 \right]^{1/2}, \quad (C-4)$$

where,

$$\frac{\delta G}{G} = \left[\left(\frac{0.01 \dot{m}}{\dot{m}} \right)^2 + \left(2 \frac{\delta D_i}{D_i} \right)^2 \right]^{1/2}, \quad (C-5)$$

$$\frac{\delta G}{G} = \left[(.01)^2 + \left(\frac{.00013}{.013157} \right)^2 \right]^{1/2} = 0.013.$$

Since $\delta u = 0.15 \text{ kg/m} \cdot \text{hr}$, then

$$\frac{\delta Re}{Re} = \left[(.013)^2 + \left(\frac{0.15}{3.1218} \right)^2 + \left(\frac{.00051}{.013157} \right)^2 \right]^{1/2} = 0.05$$

$$Re = 16102 \pm 805$$

The probable error in the coefficient C_i is given by:

$$\frac{\delta C_i}{C_i} = \left[\left(\frac{\delta D_o}{D_o} \right)^2 + \left(\frac{\delta \text{slope}}{\text{slope}} \right)^2 + \left(\frac{\delta k}{k} \right)^2 \right]^{1/2}, \quad (C-6)$$

where:

$$\delta D_o = 0.00025 \text{ m},$$

$$\delta k = 0.03 \text{ W/m} \cdot ^\circ\text{C}, \text{ and}$$

$$\delta \text{slope} = 0.065 \text{ slope}$$

$$\frac{\delta C_i}{C_i} = \left[\left(\frac{0.00025}{0.15875} \right)^2 + (.065)^2 + \left(\frac{0.03}{0.6221803} \right)^2 \right]^{1/2}$$

$$\frac{\delta C_i}{C_i} = 0.082$$

$$\underline{C_{i,15\%} = 0.026 \quad 0.002}$$

Using the above information, the probable error in the inside heat transfer coefficient can be calculated as:

$$\begin{aligned} \frac{\delta h_i}{h_i} = & \left[\left(\frac{.030}{.6221803} \right)^2 + \left(\frac{0.00051}{.0131875} \right)^2 + (.082)^2 + (0.8 \times 0.05)^2 \right. \\ & \left. + \left(\frac{.333 \times 0.1}{7.18345} \right)^2 + \left(\frac{.14 \times 0.05}{1.7645778} \right)^2 \right]^{1/2} \end{aligned}$$

$$\frac{\delta h_i}{h_i} = 0.110$$

$$\underline{h_{i,15\%} = 5896 \pm 651 \text{ W/m}^2 \text{ } ^\circ\text{C}}$$

C.3. The Uncertainty in the Outside Heat Transfer Coefficient, h_o

The probable error in the outside heat transfer coefficient is given by:

$$\begin{aligned} \frac{\delta h_o}{h_o} = & \left[\left(\frac{\delta U_n}{U_n^2 \left(\frac{1}{U_n} - R_w - \frac{D_o}{D_i h_i} \right)} \right)^2 + \left(\frac{\delta R_w}{\left(\frac{1}{U_n} - R_w - \frac{D_o}{D_i h_i} \right)} \right)^2 \right. \\ & \left. + \left(\frac{\left(\frac{D_o}{D_i h_i} \right) \left(\frac{\delta h_i}{h_i} \right)}{\left(\frac{1}{U_n} - R_w - \frac{D_o}{D_i h_i} \right)} \right)^2 \right]^{1/2} , \end{aligned} \quad (C-7)$$

where:

$$\frac{\delta U_n}{U_n} = 0.18$$

$$\delta R_w = 1.54 \times 10^{-6} \text{ m}^2 \text{ }^\circ\text{C/W, and}$$

$$\frac{\delta h_i}{h_i} = 0.110$$

Also,

$$\frac{1}{U_n} - R_w - \frac{D_o}{D_i h_i} = 9.535 \times 10^{-5} \text{ m}^2 \text{ }^\circ\text{C/W}$$

With this information

$$\begin{aligned} \frac{\delta h_o}{h_o} = & \left[\left(\frac{0.181}{(2996)^2 (9.535 \times 10^{-5})} \right)^2 + \left(\frac{1.54 \times 10^{-6}}{9.535 \times 10^{-5}} \right)^2 \right. \\ & \left. + \left(\frac{(.015875)(.096)}{(.0131575)(5896)(9.535 \times 10^{-5})} \right)^2 \right]^{1/2} \end{aligned}$$

$$\frac{\delta h_o}{h_o} = 0.207$$

$$\underline{h_o = 10,338 \pm 2152 \text{ W/m}^2 \text{ }^\circ\text{C}}$$

BIBLIOGRAPHY

1. Search, H. T., A Feasibility Study of Heat Transfer Improvement in Marine Steam Condensers, MSME, Naval Postgraduate School, Monterey, CA, December 1977.
2. Bromley, L. A., et al., "Promotion of Drop-By-Drop Condensation of Steam from Seawater on a Vertical Copper Tube," AIChE Journal, Vol. 14, No. 2, March, 1968, p. 245-250.
3. Osment, B. D. J., et al., "Promoters for the Dropwise Condensation of Steam," Institution of Chemical Engineers, Transactions, Vol. 40, 1962, p. 152-160.
4. Erb, R. A., and Thelen, E., Dropwise Condensation Characteristics of Permanent Hydrophobic Systems, Franklin Institute, Philadelphia, PA, Office of Saline Water, Research and Development Progress Report No. 184, April 1966.
5. Wilkins, D. G., and Bromley, L. A., "Dropwise Condensation Phenomena," AIChE Journal, Vol. 19, No. 4, July 1973, p. 839-845.
6. Smith, G. F., Promotion of Dropwise Condensation by Teflon Coated Condenser Tubes, U. S. Naval Engineering Experiment Station, Annapolis, MD, Evaluation Report 030038B, NS-643-078, 12 October 1956.
7. Cox, E. F., Investigation of the Use of Non-Wetting Agents for Promoting Dropwise Condensation on Steam Condenser Tubes, Westinghouse Electric Corporation, Lester Works, Heat Transfer Department, Engineering Memo EM-377, 19 May 1959.
8. Heat Transfer Rates of Teflon-Coated Condenser Tubes, U. S. Naval Engineering Experiment Station, Annapolis, MD, Evaluation Report 720038D, S-F13 08 15-4199, 7 November 1960.
9. Depew, C. A., and Reisbig, R. L., "Vapor Condensation on a Horizontal Tube Using Teflon to Promote Dropwise Condensation," I & EC Process Design and Development, Vol. 3, No. 4, October 1964, p. 365-369.
10. Erb, R. A., and Thelen, E., "Dropwise Condensation," First International Symposium on Water Desalination, Washington, D. C., 3-9 October 1965.

11. Tanasawa, I., "Dropwise Condensation: The Way to Practical Applications," Sixth International Heat Transfer Conference, Vol. 6, Toronto, Canada, August 1978, pp. 383-407.
12. Croix, J. M., and Liegeois, A., Condensation in a Horizontal Tubular Bundle, Department of Transfer & S.E.T.R.E., Report of Tests, TT/SETRE/78-3-B/JMC, ALi, 8 March 1978.
13. Beck, A. C., A Test Facility to Measure Heat Transfer Performance of Advanced Condenser Tubes, MSME, Naval Postgraduate School, Monterey, CA, December 1976.
14. Pence, D. T., An Experimental Study of Steam Condensation on a Single Horizontal Tube, MSME, Naval Postgraduate School, Monterey, CA, March 1978.
15. Fenner, J. H., An Experimental Comparison of Enhanced Heat Transfer Condenser Tubing, MSME, Naval Postgraduate School, Monterey, CA, September 1978.
16. Reilly, D. J., An Experimental Investigation of Enhanced Heat Transfer on Horizontal Condenser Tubes, MSME, Naval Postgraduate School, Monterey, CA, March 1978.
17. Griffith, J. R., Personal Correspondence, 6120-375: JRG: mjt, Naval Research Laboratory, Washington, D. C., 30 August 1978, 2p.
18. "Nedox," General Magnaplate Corporation pamphlet, Linden, NJ, 1972, 2 p.
19. "Tufram," General Magnaplate Corporation pamphlet, Linden, NJ, 1974, 4 p.
20. "Canadizing," General Magnaplate Corporation pamphlet, Linden, NJ, 1 p.
21. Holman, J. P., Heat Transfer, 4th ed., McGraw-Hill, 1976.
22. Wilson, E. E., A Basis for Rational Design of Heat Transfer Apparatus, paper presented at the Spring Meeting of the Society of Mechanical Engineers, Buffalo, NY, June 1935.
23. Briggs, D. E., and Young, E. H., "Modified Wilson Plot Techniques for Obtaining Heat Transfer Correlations for Shell and Tube Heat Exchangers," Heat Transfer-Philadelphia, v. 65, No. 92, 1969, p. 35-45.

24. Subroutine, NPS COMPUTER FACILITY, LEAST SQUARES POLYNOMIAL FITTING, LSQPL2, Programmed by D. E. Harrison, November 1969.
25. Graham, C., The Limiting Heat Transfer Mechanisms of Dropwise Condensation, PhD Thesis, Massachusetts Institute of Technology, March 1969.
26. Stylianou, S. A. and Rose, J. W., "Dropwise Condensation on Surfaces Having Different Thermal Conductivities," paper at Queen Mary College, University of London, 25 p.
27. Mikic, B. B., "On Mechanism of Dropwise Condensation," International Journal of Heat and Mass Transfer, Vol. 12, 1969, p. 1311-1323.
28. Kline, S. J. and McClintock, F. A., "Describing Uncertainties in Single Sample Experiments," Mechanical Engineering, V. 74, pp. 3-8, January 1953.

INITIAL DISTRIBUTION LIST

	No. Copies
1. Defense Documentation Center Cameron Station Alexandria, Virginia 22314	2
2. Library, Code 0142 Naval Postgraduate School Monterey, California 93940	2
3. Department Chairman, Code 69 Department of Mechanical Engineering Naval Postgraduate School Monterey, California 93940	2
4. Office of Research Administration, Code 012A Naval Postgraduate School Monterey, California 93940	1
5. Professor Paul J. Marto, Code 69Mx Department of Mechanical Engineering Naval Postgraduate School Monterey, California 93940	20
6. LT John T. Manvel, Ur. Supervisor of Shipbuilding, Conversion and Repair, USN Newport News, Virginia 23607	4
7. CDR W. W. Baline, USN Naval Sea Systems Command (033) (acting) 2221 Jefferson Davis Highway, CP#6 Arlington, Virginia 20360	1
8. Mr. Charles Miller Naval Sea Ssystems Command (0331) 2221 Jefferson Davis Highway, CP#6 Arlington, Virginia 20360	2
9. Mr. Frank Ventriglio Naval Sea Systems Command (0331) 2221 Jefferson Davis Highway, CP#6 Arlington, Virginia 20360	1
10. Dr. Earl Quandt Naval Ship Research & Development Center Annapolis Laboratory Annapolis, Maryland 21402	1

11. Mr. J. W. Murrin 1
Naval Seas Systems Command (0331)
2221 Jefferson Davis Highway, CP#6
Arlington, Virginia 20360
12. CAPT R. E. Greer, USN 1
Naval Sea Systems Command (PMS-301)
2221 Jefferson Davis Highway, CP#6
Arlington, Virginia 20360
13. CDR D. W. Barns, USN 1
Naval Sea Systems Command (PMS-301.B)
2221 Jefferson Davis Highway, CP#6
Arlington, Virginia 20360
14. Mr. Walter Aerni 1
Naval Ship Engineering Center (6145)
Washington, D. C. 20360
15. Mr. Wayne L. Adamson 1
Naval Ship Research & Development Center (2761)
Annapolis, Maryland 21402
16. Mr. Gil Carlton 1
Naval Ship Engineering Center (6723)
Philadelphia, Pennsylvania 19112
17. Dr. David Eissenberg 1
Oak Ridge National Laboratory
Post Office Box Y
Oak Ridge, Tennessee 37830
18. Miss Eleanor J. Macnair 1
Ship Department
Ministry of Defence
Director - General Ships, Block B
Foxhill, Bath, Somerset
ENGLAND
19. Mr. Kurt Bredehorst 1
NAVSEC 6147D
Department of the Navy
Hyattsville, Maryland 02782
20. Professor Kenneth J. Bell 1
School of Chemical Engineering
Oklahoma State University
Stillwater, Oklahoma 74074
21. Professor A. E. Bergles 1
Department of Mechanical Engineering
Iowa State University
Ames, IA 50010

22. Professor James G. Knudsen 1
Engineering Experimental Station
Oregon State University
Covell Hall-219
Corvallis, Oregon 97331
23. Dr. Ken Read 1
OTEC Branch
Division of Solar Energy
Department of Energy
Washington, D. C. 20545
24. Dr. A. L. London 1
4020 Amaranta Avenue
Palo Alto, California 94306
25. Mr. Norman F. Sather 1
Argonne National Laboratory
9700 S. Cass Avenue
Argonne, Illinois 60439
26. Dr. Jeff Horowitz 1
Argonne National Laboratory
9700 S. Cass Avenue
Argonne, Illinois 60439
27. Mr. M. K. Ellingsworth 1
Office of Naval Research
800 N. Quincy Street
Arlington, Virginia 22217
28. Mr. R. Muench 1
David W. Taylor Naval Ship Research
and Development Center
Annapolis Laboratory
Annapolis, Maryland 21402
29. Mr. W. Thielbar 1
Naval Weapons Center
China Lake, California 93555
30. CAPT Bress (Code 03) 1
Naval Sea Systems Command
Washington, D. C. 20362
31. Mr. John Michele 1
Oak Ridge National Laboratory
Oak Ridge, Tennessee 37830
32. Dr. Win Aung 1
Division of Engineering, National Science
Foundation
1800 "G" Street NW
Washington, D. C. 20550

- | | | |
|-----|-----------------------------------|---|
| 33. | Mr. John W. Ward | 1 |
| | Marine Division | |
| | Westinghouse Electric Corporation | |
| | Hendy Avenue | |
| | Sunnyvale, California 94088 | |
| 34. | Dr. James Griffith | 1 |
| | Chemistry Division | |
| | Naval Research Laboratory | |
| | Washington, D. C. 20550 | |
| 35. | Dr. Theodore Corvino | 1 |
| | General Magnaplate Corporation | |
| | 1331 US Route 1 | |
| | Linden, New Jersey 07036 | |

